PHYSICAL REVIEW D VOLUME 46, NUMBER 6 15 SEPTEMBER 1992

# Bubble nucleation and growth at a baryon-number-producing electroweak phase transition

Bao Hua Liu and Larry McLerran
*Theoretical Physics Institute, University of Minnesota, Minneapolis, Minnesota 55455*

Neil Turok*
*Blackett Laboratory, Imperial College, London S.W. 7, United Kingdom*
(Received 1 May 1992)

We discuss the nucleation and growth of bubbles of the broken-symmetry phase of matter at the electroweak phase transition. We show that the bubble walls propagate with a mildly relativistic speed. The Lorentz $\gamma$ factor depends on the ratio of the Higgs to gauge-boson mass—for parameters allowing for baryogenesis at the transition (i.e., a fairly light Higgs mass) we find $\gamma v \sim 1$. We show that the bubble wall is mainly slowed by interactions with low-momentum gauge-boson pairs, and compute the damping rate due to these interactions. The width of the bubble wall is significantly larger than the typical wavelength of particles which are reflected from it, which allows us to use a WKB approximation for the particle scattering. The width is also larger than the mean free path for these particles, which means that the gauge boson fluid remains close to local thermal equilibrium. This situation results in mildly relativistic motion of the bubble wall. As a result, the baryon-number excess produced on the bubble wall is not much diluted by subsequent diffusion. We compute the effective equation of motion for the Higgs field, and the approximate shape of the moving bubble wall.

PACS number(s): 12.15.Ji, 98.80.Cq

## I. INTRODUCTION

Since the work of 't Hooft [1], it has been known that the rate for baryon-number violation in electroweak theory is nonzero. Early work on this problem led to the suggestion that baryon-number violation might proceed at a reasonable rate at high temperature or high energy [2–5]. Only recently has it been convincingly argued that the rate is large at high temperature [6,7], and the situation in high-energy collisions is still completely unclear [8]. Detailed calculations [9] have shown that, at temperatures larger than about 100 GeV, the rate for baryon-number violation in the standard electroweak theory is large enough to substantially affect the baryon asymmetry of the Universe.

This raises the exciting possibility that the observed baryon asymmetry of the Universe was created at temperatures of order 100 GeV, through electroweak physics which should be experimentally accessible within the foreseeable future. Since the electroweak theory is a weak-coupling theory, it should be possible to perform an *ab initio* calculation of the baryon asymmetry, taking the standard hot-big-bang nucleosynthesis calculations of the abundances of the light elements an important step back in time, and explaining the value of the one adjustable parameter in those calculations, the baryon-to-photon ratio.

The conditions for generating a baryon asymmetry in the big bang were pointed out long ago by Sakharov [10]. In addition to $B$ nonconservation, the universe must fall out of equilibrium and the underlying dynamics must violate $CP$. The first condition is easily satisfied in electroweak theory since the phase transition which generates masses for $W$, $Z$, and Higgs bosons is generically of first order [11–34]. $CP$ is also violated in the standard model and its extensions. Therefore, in electroweak theory, all the conditions are satisfied which would allow for the generation of a baryon asymmetry at the electroweak phase transition. It is then a matter of the detailed dynamics as to whether a baryon asymmetry of an acceptable magnitude is generated.

It has only recently been recognized that the dynamics of electroweak theory may generate the baryon asymmetry of the Universe [16–19]. Much recent activity has been stimulated since, in a variety of simple electroweak scenarios, the baryon asymmetry which is produced appears naturally to be of the same order as that which is observed in the Universe [20–23].

To refute or confirm these scenarios it is clear that a detailed understanding of the dynamics of the electroweak phase transition must be developed. While one has a relatively clear understanding of the nucleation of bubbles of the broken-symmetry phase [24,25], their subsequent evolution as they expand and sweep up the symmetric phase is much less well understood. In a recent letter, one of us (N.T.) made a start on this problem [25].

It is surprising that the bubble-growth problem in the electroweak theory was not solved long ago. At first sight, it appears to be a simple problem in hydrodynamics [26–28]. However, closer inspection shows that one must understand the microscopic details of the burning of symmetric electroweak matter into the broken-symmetry phase at the surface of the bubble. In fact, to

*On leave from the Physics Department, Princeton University, Princeton, NJ 08544.

 

compute the velocity of the propagation of the bubble wall, one must necessarily investigate microscopic entropy-producing processes [27,25].

Let us begin by reviewing the general constraints on producing and preserving a baryon asymmetry at the electroweak phase transition. Using the results of Ref. [11], it was argued in Ref. [20] that, for theories with multiple Higgs doublets, the effective potential for the Higgs fields responsible for the symmetry-breaking electroweak phase transitions takes the form

$$V(\phi)=\frac{1}{2}M^2(T)\phi^2-\delta T\phi^3+\frac{\lambda}{4}\phi^4 \tag{1}$$

where $M^2(T)\sim\frac{5}{16}g^2(T^2-T_c^2)$, and where $T_c$ is the temperature at which the curvature of the potential near the origin vanishes. The field $\phi$ here is a linear combination of the fields which at zero temperature generate the physical scalar particles. The parameter $\delta\sim(3/32\pi)g^3$. We will take this form of the potential throughout the analysis in this paper. Improvements of this potential using, for example, the method of Carrington [15–34], which includes the effects of ring diagrams and a large top-quark mass, lead to modifications of our results which are of order unity, and will be investigated fully in a later analysis.

Bubble nucleation takes place when the height of the barrier separating the minima corresponding to broken- and unbroken-symmetry phases becomes small. As the Universe cools, the nucleation rate grows until it is comparable to the expansion rate of the Universe. After the bubbles nucleate, they rapidly expand to fill space, all this occurring in a time of the order of $4\times10^{-5}$ of an expansion time [25].

In the center of the bubbles, the Higgs-field magnitude is fixed by the parameters in the Higgs potential. These must be chosen so that the rate of baryon number violation in the broken symmetry phase is small compared to the expansion rate of the Universe. This requires that, in the broken symmetry phase immediately after the transition, the sphaleron mass is large compared to the temperature. The value of the vector-boson mass for which this occurs may be estimated using the formula [7]

$$\Gamma/V=\kappa(\lambda/g^2)T^4\left[\frac{\alpha_W}{4\pi}\right]^4 N_{\rm tr}N_{\rm rot}\left[\frac{2M_W(T)}{\alpha_W T}\right]^7 \times\exp[-E_S(T)/T]\ . \tag{2}$$

In this equation, $\kappa(\lambda/g^2)$ is a function of the Higgs self-coupling scaled by the gauge coupling squared, which must be numerically evaluated [9]. The factors of $N_{\rm tr}$ and $N_{\rm rot}$ are zero-mode factors evaluated in Ref. [9]. The factor $E_S(T)$ is the mass of the sphaleron whose value is

$$E_S(T)=\frac{2M_W(T)}{\alpha_W}A(\lambda/g^2)\ , \tag{3}$$

where $1.5<A<2.7$ for $0\le\lambda/g^2\le\infty$. For the one-doublet theory, $A$ is very close to 1.5 for the light Higgs mass we use. Needless to say, in the two-doublet theory, $A$ may be slightly different.

Using this formula, and requiring that the sphaleron rate be smaller than the cooling rate (the expansion rate of the Universe $\sim T/m_{\rm Pl}\sim e^{-40}$), implies a constraint on the gauge-boson mass,

$$M_W(T)\ge 15\alpha_W T\ . \tag{4}$$

This must be satisfied if a baryon asymmetry produced via anomalous processes is to be preserved after the phase transition.

In the unbroken symmetry phase, the rate of $B+L$ violation is large

$$\Gamma\sim\alpha_W^4T^4\ . \tag{5}$$

As one passes through the bubble wall, however, the effective mass of the gauge bosons grows, and the rate for $B+L$ violation decreases. Comparing Eqs. (2) to (5), one finds that the region of the bubble wall for which baryon number violation is turned on has

$$M_W\le 7\alpha_W T\ . \tag{6}$$

However, this simple picture, in which the sphaleron processes occur at the thermal equilibrium rate appropriate to the local value of $M_W$ in the bubble wall, is certainly too naive—a recent numerical study in $1+1$ dimensions indicates that the relaxation to the vacuum behind propagating bubble walls is inherently a far-from-equilibrium process [31], with $B+L$ violation actually being driven by energy stored in the unbroken-symmetry vacuum. Nevertheless, it is still true that $(B+L)$-violating processes are turned off as one passes through the bubble wall.

The bound of Eq. (4), the requirement that one preserve any baryons created by processes occurring in the bubble wall, imposes a strong constraint on the effective potential for the Higgs field. As we shall see in the next section, the Higgs-field expectation value just after the transition is completed is close to the value where the minima of the potential are degenerate. We therefore have

$$\phi(T)=2\frac{\delta}{\lambda}T=\frac{3g^3}{16\pi\lambda}T \tag{7}$$

or, using Eq. (4),

$$\frac{g^2}{\lambda}\ge 40\ . \tag{8}$$

This is the same as

$$M_H^2/M_W^2\le 0.2 \tag{9}$$

where we have used the Higgs boson mass $M_H=\sqrt{2\lambda}\phi$ at zero temperature, and the vector boson mass $M_W=g\phi/2$. Note that we use the value of $\phi(T)$ at the transition, which occurs well before the metastable minimum disappears. This makes the upper bound on the Higgs mass lower by a factor $\sqrt{2/3}$, a substantial effect—Eq. (9) corresponds to $M_H\le 35$ GeV. Previous treatments of the one-doublet [16] and two-doublet [13,14] models have not properly taken this into account.

Strictly speaking, this is the Higgs mass at zero tem-

perature only in the standard one-doublet model. In multiple-doublet models, in which *CP* violation in the Higgs sector drives baryogenesis, there is no simple relation—at zero temperature, $M_H/M_W \neq 2\sqrt{2\lambda}/g$. For our purposes, it is useful to think of this ratio of couplings in terms of a Higgs boson mass which would be the naive zero-temperature limit of the finite-temperature theory, and remember that the limits on what we call the Higgs mass are not those for any physical particle. The effective bound on the mass of the lightest physical scalar in the two-doublet model, for example, is weaker, but only by a factor of 2 or so [14]. We shall for simplicity stick to the one-doublet model throughout this paper, although it is to be regarded as merely a convenient parametrization of the Lagrangian for the multiple-Higgs-doublet models we are more interested in for baryogenesis.

The one-doublet model seems to be ruled out for baryogenesis, because there is a lower bound on the ratio (9) from recent CERN LEP experiments, which set a bound $M_H > 57$ GeV. This corresponds to $M_H(0)^2/M_W(0)^2 > 0.48$, which clearly conflicts with Eq. (9). *CP* violation in the one-doublet theory also appears much too small to make the observed asymmetry—we shall return to this point, and the interesting recent scenario of [23] below. In more complicated multiple-Higgs-doublet models, in which there is *CP* violation in the Higgs potential, and therefore a better prospect for generating a baryon asymmetry [19,20], there is more room to maneuver and avoid the experimental constraint. In order to preserve the baryon asymmetry, there is a limit on the lightest-mass Higgs boson, just as in the one doublet model, but the upper limit is of order $M_H \leq 125$ GeV [13,14] (although this may be a little too high, because of the factor of $\sqrt{2/3}$ mentioned above). In the regime of interest in these theories, the potential is quite similar to the one-doublet potential with the Higgs mass close to the experimental limit. We shall therefore take as a reasonable "realistic" range of values

$$M_H^2/M_W^2 \sim 0.2\text{–}0.4 \tag{10}$$

(corresponding to 35 GeV $< M_H <$ 50 GeV, $0.01 < \lambda < 0.02$) of course remembering that in extended models $M_H$ is not the true zero-temperature value of the Higgs mass.

The naive "equilibrium" picture of baryon number violation inside the bubble wall is that for $M_W(T) \leq 7\alpha_W T$ the sphaleron transitions are strongly turned on. For $7\alpha_W T \leq M_W(T) \leq 15\alpha_W T$, the sphaleron rates are shutting off, and by the time one reaches the value $M_W(T) \geq 15\alpha_W T$, the rate of sphaleron transitions is slower than the expansion rate of the Universe. In order to evaluate the amount of baryon-number violation during the evolution of the bubble wall, one must translate these mass ranges into length scales within the bubble wall. Since the ratio of mass scales when the sphaleron rate is large to that when it shuts off is of order 1, and the value at which it shuts off is close to the vacuum value, we expect that the ratio of scales in the bubble wall is of order unity. We shall also see that the size of the bubble wall is of the order of the sphaleron size $L \sim M_H(T)^{-1} \sim 1/(\alpha_W T)$, so that the region where the baryon number violation is strong in the bubble is of the order of a typical sphaleron size.

The velocity of the bubble wall is crucial for two reasons. First, if the bubble wall is moving fast then its width is Lorentz contracted, and when it passes by the sphalerons its effect should be localized and small. One might reasonably expect some suppression of the effect the wall has in biasing the baryon-number-changing processes.

The second reason is that if the wall moves too slowly, diffusion may erase the baryon asymmetry as it is produced. The baryon asymmetry produced on the bubble wall may diffuse out into regions where the baryon number is rapidly violated, and be destroyed—outside the bubble, and in the outer part of the bubble wall, the rate of baryon number changing process is large. If we imagine following a quark or lepton carrying $B+L$ across the bubble wall into the unbroken symmetry phase, there is a characteristic time for it to last before it participates in a $(B+L)$-violating event, and the $B+L$ it carries is destroyed. This is given by

$$t_B \sim 1/(\alpha_W^4 T) \tag{11}$$

since the total rate of $(B+L)$-violating processes is given by (5) and the number density of particles involved is $\sim T^3$. Alternatively, one may compute the chemical potential corresponding to a small excess of $B+L$, and calculate the resulting bias in the $(B+L)$-violating processes, whose total rate is given by (5). One then finds that $T_B$ is the relaxation time for a $B+L$ excess in the unbroken symmetry phase.

$B+L$ diffuses outward since the effect of the chemical potential of the baryons produced by the wall is to make a potential difference for baryon number. Assuming that the process is diffusive, we may therefore estimate the minimum velocity of the bubble walls above which diffusion will play little role. During one characteristic $(B+L)$-violation time $t_B$, the wall must move a distance $(vt_B)$ large than the typical diffusion length. The diffusion length is

$$d \sim \sqrt{\lambda t_B} \tag{12}$$

where $\lambda$ is the quark or lepton mean free path, much less than $t_B$. The quark mean free path is determined by strong scattering,

$$\lambda \sim \frac{1}{\alpha_S^2 T} \tag{13}$$

since the number density of quarks $n \sim T^3$, and the cross section $\sigma \sim \alpha_S^2/T^2$. The lepton mean free path is larger,

$$\lambda \sim \frac{1}{\alpha_W^2 T} \ . \tag{14}$$

To preserve the $B+L$ created by the wall, it follows that a sufficient condition is that

$$v_{\text{wall}} > d/t_B \sim \alpha_W \ . \tag{15}$$

We shall find that this condition is satisfied in the realistic case, so the baryon asymmetry is not erased by diffusion.

In this paper, we will describe in some detail the structure of nucleation bubbles propagating into the electroweak plasma. We shall find that the velocity of the wall is faster than that for which diffusion is important but slow enough so that it is only mildly relativistic, and the baryon-number-violating dynamics should not be very drastically affected.

There is still a good deal of uncertainty regarding the detailed calculation of the final baryon asymmetry in the various scenarios which have been proposed. The estimates of [20] for example, are certainly quite crude. In that paper, it was shown that two different ways of looking at the process—as a biasing of a close-to-equilibrium rate for $B+L$ violation or as a perturbation to the classical equations of motion where the $CP$-violating Higgs potential drives the baryon asymmetry in a completely deterministic manner—gave the same estimate for the final asymmetry. Recent $(1+1)$-dimensional simulations support the latter viewpoint—the process of baryon number violation appears to be intrinsically a nonequilibrium phenomenon [31], and they confirm the magnitude of the earlier estimate. However, these simulations only include bubble walls very crudely, and it is clear that understanding the dynamics of the bubble wall is a very important first step towards a detailed microscopic computation of the baryon asymmetry.

In scenarios such as those recently advocated in Refs. [22,23], the baryon-number violation takes place in a region whose size is of the order of a typical particle mean free path around the bubble-wall surface. These scenarios require that the bubble wall have a thickness much less than a particle wavelength and that the size of the diffusion region associated with particle scattering be large compared to the bubble-wall thickness. The typical wavelength, which is important for the scenarios above, is of order $1/M(T)$, where $M(T)$ is a $W$-boson mass at the temperature near the transition temperature. We shall see that these scenarios must be greatly modified since the typical bubble-wall thickness is about an order of magnitude larger than the typical particle wavelength and very much greater than a quark mean free path. (In some models of electroweak dynamics, it may be possible to adjust parameters in such a way that the bubble wall is thin, and arrange the temperature of the transition to be sufficiently low so that the mean free paths are large. Such an adjustment we regard as possible but not natural, and will not further consider it [29].)

The outline of this paper is as follows. In Sec. II, we briefly review the nucleation process which generates the bubbles. We compute the value of the Higgs field and the temperature at which the nucleation rate is fast enough to fill the universe with a region of the stable broken-symmetry phase of electroweak theory.

In Sec. III, we discuss the gross features of bubble growth. In particular, we discuss bubble growth in the case of slow burning, that is deflagrations, and for rapid burning or detonations. We argue that the out-of-equilibrium processes which generate entropy are important in determining the speed at which the bubble wall propagates. We also discuss the shape of the bubble wall.

In Sec. IV, we discuss the equation which determines the velocity of the bubble wall. In order that the wall have a finite terminal velocity, damping forces must arise which slow the bubble wall, since otherwise it would accelerate to arbitrarily close to the speed of light. This is because the phase transition releases energy, and in the absence of damping, all of the energy released would go into the kinetic energy of the bubble wall. We shall argue that the dominant term which generates the damping arises from a buildup of $W$-and $Z$-boson pairs in the vicinity of the wall.

In Sec. V, we compute the damping of the bubble wall in an unrealistic, but instructive, approximation where we assume that the mean free path for particle scattering is large compared to the width of the bubble wall. We use a WKB approximation, and show that in this limit our computation has the simple interpretation of a pressure generated by scattering from the wall of particles whose masses change as one passes through the wall.

In Sec. VI, we compute the damping on the wall in the realistic limit when the mean free path is small compared to the size of the bubble wall. We discuss the relevant mean free paths, and a general formalism for solving the Boltzmann transport equation for the perturbed phase-space density, which in the end is what determines the bubble-wall terminal propagation speed. We compute the deviations from equilibrium distribution functions, and their effect on the damping of the bubble wall. We find that parametrically for small coupling, the Lorentz $\gamma$ factor for the bubble wall depends only on the ratio of Higgs- to $W$-boson masses. We find that the bubble wall Lorentz $\gamma$ factor $\sim 1$, but do not at present have a sufficiently good computation to determine whether or not the bubble propagates as a detonation or a deflagration.

In Sec. VII, we discuss our results and compare them to earlier attempts to compute the terminal velocity of bubbles in the electroweak plasma.

## II. THE NUCLEATION PROCESS AND GROSS FEATURES OF BURNING

The nucleation process in cosmology for a potential of the type given in Eq. (1) was outlined in Refs. [24,12] and applied to the electroweak theory in [20–25]. We will expand a little on that analysis here. We will review the computation of the bubble action, and use this to determine the temperature when the entire Universe is converted into the asymmetric phase. This will be needed in our later analysis. We shall also discuss a simple variational ansatz, and a numerical fit which allows for a good approximate analytic computation of the nucleation rate.

From the analysis of Refs. [24,12], the rate of bubble nucleation per unit volume is given by

$$\Gamma = M^4(T)\left[\frac{S_3}{\pi T}\right]^{3/2} e^{-S_3/T} \tag{16}$$

where $S_3$ is the three-dimensional O(3)-invariant bubble action and $M^2(T)=\gamma(T^2-T_c^2)$ as below.

Recall that the effective potential for the electroweak theory from Eq. (1) may be written as

$$V(\phi)=\frac{\gamma}{2}(T^2-T_c^2)\phi^2-\delta T\phi^3+\frac{\lambda}{4}\phi^4 \tag{17}$$

where $\phi=\sqrt{2}(\Phi^\dagger\Phi)^{1/2}$, with $\Phi$ the standard Higgs doublet field and

$$\gamma=\tfrac{1}{4}(2M_W^2+M_Z^2+2M_t^2)/\phi_0^2\sim\tfrac{5}{16}g^2$$

when $M_W\sim M_Z\sim M_t$, and $M_t$ is the top-quark mass. The parameter $\delta$ was defined previously and is

$$\delta=\frac{2M_W^3+M_Z^3}{4\pi\phi_0^3}\sim\frac{3}{32\pi}g^3 .$$

Throughout this paper, we will assume that the top-quark mass is of the order of the $W$- and $Z$-boson masses. Corrections to this should be computed using the method of Carrington [15–34], but for our semiquantitative analysis this will not be done. We will also assume a light Higgs-boson mass, i.e., $\lambda$ is small, $g^4\ll\lambda\ll g^2$, as discussed in Sec. I.

Following Turok [25], we re-express the effective potential in terms of a dimensionless temperature $\zeta=\chi(1-T_c^2/T^2)$, where $\chi=\lambda\gamma/\delta^2\gg1$. Notice that for large temperatures, $\zeta$ is large. At $T_c$, corresponding to a massless scalar particle in the effective potential, $\zeta=0$. As $\zeta$ is decreased from large positive values, the effective potential at first has only one minimum centered at $\phi=0$. At $\zeta=2.25$, a second relative but not absolute minimum develops at nonzero $\phi$. At $\zeta=2.00$, the minimum at $\phi=0$ and nonzero $\phi$ become degenerate, and at smaller values of $\zeta$ the system is unstable with respect to decay into the system with a nonzero value of $\phi$. At $\zeta=0$, the local minimum at $\phi=0$ disappears, and there is no barrier which prevents decay into the asymmetric phase. At this temperature, the system would spinodally decompose if it had not already undergone a first-order phase transition. This would happen only with a large cooling rate—in the electroweak transition, the cooling rate is the expansion rate of the Universe, and is very slow.

We now must compute the bubble nucleation rate. The critical bubble action is the stationary point of the three-dimensional action functional. It represents the free-energy barrier to the creation of a macroscopic region of broken symmetry phase. It is a maximum with respect to changes in the size of the bubble, so that smaller bubbles collapse, but larger bubbles grow. It is a minimum with respect to other changes, however, so it is a classical solution with one unstable mode. To calculate the bubble action, it is convenient to express it in terms of a dimensionless radius, $x=(\delta/\sqrt{\lambda})Tr$, and a dimensionless field strength $g=(\lambda/\delta T)\phi$. We will assume an O(3)-symmetric bubble gives the stationary three-dimensional action which interpolates between the phases, so that

$$S_3/T=4\pi\left[\frac{\delta^2}{\lambda^3}\right]^{1/2}\times\int x^2dx\left[\frac{1}{2}\left[\frac{dg}{dx}\right]^2+\left[\frac{1}{4}g^4-g^3+\frac{\zeta}{2}g^2\right]\right] \tag{18}$$

so the bubble action is proportional to $\sqrt{\delta^2/\lambda^3}$ times a function only of $\zeta$.

The three-dimensional action has been computed numerically by Turok [25]. We will expand upon that analysis here. In the relevant regime, the "thin-wall" approximation is not good, but a Gaussian approximation is reasonable.

To begin with, we use the following Gaussian ansatz,

$$g(x)=g_0e^{-x^2/x_0^2} \tag{19}$$

where $g_0$ and $x_0$ are the two variational parameters. It is straightforward to compute the bubble action and extremize with respect to $g_0$ and $x_0$. The result is that (18) is given by

$$S_3/T=\frac{\pi^{3/2}}{\zeta^{3/2}}\left[\frac{\delta^2}{\lambda^3}\right]^{1/2}\left[\frac{1}{2^{5/2}}(3+l^2)lg_0^2\zeta+g_0^3l^3\left[\frac{g_0}{32}-\frac{1}{3^{3/2}}\right]\right], \tag{20}$$

where the dimensionless size of the bubble $x_0=l/\zeta^{1/2}$, with $l$ given by

$$l=\frac{1}{[1-(2/3)^{3/2}g_0/\zeta]^{1/2}} \tag{21}$$

and the value of the field at the center of the bubble given by

$$g_0=\frac{8}{\sqrt{3}}\left[1-\left[1-\frac{3\zeta}{4\sqrt{2}}\right]^{1/2}\right] . \tag{22}$$

This ansatz works well for $\zeta<1.5$ or so, and gives the small-$\zeta$ dependence found by Linde [24]

$$S_3/T\sim\frac{3\sqrt{3}\pi^{3/2}}{2^{5/2}}\frac{\delta}{\lambda^{3/2}}\zeta^{3/2}\quad\text{for }\zeta\to0 \tag{23}$$

with the coefficient approximately 5% higher than Linde's numerical result. Unfortunately, the Gaussian ansatz fails as $\zeta$ approaches 1.68 from below, since $x_0$ diverges.

The true solution begins to approach the "thin-wall" behavior beyond this point, which is described for example in [24]. The idea is that the bubble should be composed of an interior, in which $\phi$ takes the false-vacuum value, and a wall, within which $\phi$ interpolates from the false to the true vacuum. The energy per unit area of the wall is taken to be that of the static domain-wall solution to the theory at $\zeta=2$, when the two vacua are degenerate. The sole variational parameter is the radius of the bubble. Extremizing, one finds

$$S_3/T=4\pi\left[\frac{\delta^2}{\lambda^3}\right]^{1/2}\frac{8^{3/2}}{81}\frac{1}{(2-\zeta)^2}\ . \tag{24}$$

The dimensionless radius of the bubble is given by $x=(\sqrt{8}/3)(2-\zeta)^{-1}$.

We have plotted he results of the Gaussian approximation, the "thin wall" approximation, and an accurate numerical calculation in Fig. 1. The region of interest is around $\zeta\sim 1.6$, where it is seen that neither are particularly good. Over the interval $1.3<\zeta<1.8$, the numerical results are well approximated by [25]

$$S_3/T=\left[0.13\left[\frac{\delta^2}{\lambda^3}\right]\right]^{1/2}\frac{C}{(2-\zeta)^a} \tag{25}$$

where $C=30$, $a=1.6$ and the factor in square brackets is unity for $M_H=50$ GeV, our "realistic" case.

If the bubbles grow at a speed $v$, then the fraction of the Universe remaining in the unbroken phase at a time $t$ is given by

$$f_U=\exp\left[-\int_0^t dt'\frac{4\pi}{3}v^3(t-t')^3\Gamma(t')\right] \tag{26}$$

with $t$ the cosmic time. To a good approximation the time dependence of the prefactor in $\Gamma$ may be ignored,

$$\Gamma\approx t_c^{-4}(m_{\rm Pl}/T_c)^4\exp(-S_3/T)$$
$$\approx t_c^{-4}\exp(160-S_3/T)\ .$$

Now change variables to

$$\zeta=\chi(1-T_c^2/T^2)=\chi(1-t/t_c)$$

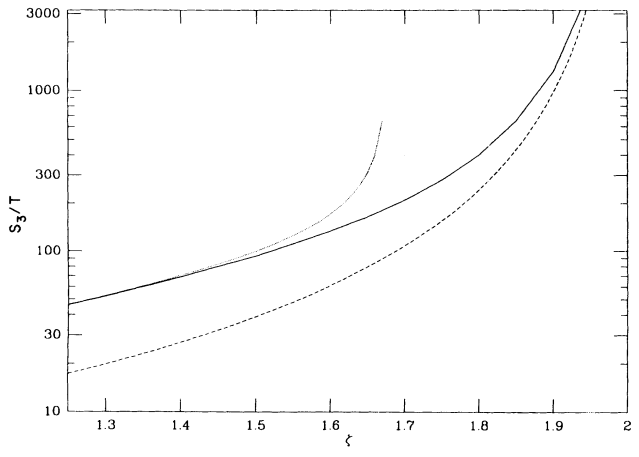


FIG. 1. The bubble free energy $S_3/T$ plotted against the dimensionless temperature $\zeta$ defined in the text. The solid line shows the results of an accurate numerical evaluation. The dotted line shows the results based on a Gaussian ansatz for the field profile, and the dashed line the results of the "thin-wall" approximation. At $\zeta=2$, the broken-symmetry vacuum becomes degenerate with the unbroken-symmetry vacuum. The bubble action is infinite. As the Universe cools, the bubble action falls. The phase transition happens around $\zeta=1.6$. These results correspond to $M_H=50$ GeV, or $\lambda^3/\delta^2=0.13$.

and expand $S_3/T$ about the point where it equals 160, $S_3/T(\zeta')\approx 160+D(\zeta'-\zeta_0)$, with $\zeta_0\approx 1.65$ and $D=160a/(2-\zeta_0)\approx 730$. The phase transition occurs close to this point. The $\zeta'$ integral is dominated by a saddle point, and the exponent in (26) grows to unity at a value of $\zeta\approx\zeta_0+D^{-1}\ln[v^3/(D_\chi)^4]\approx 1.6$. As noted in [25], at this value of $\zeta$, there is no possibility of phase coexistence, and the system converts entirely to the asymmetric phase of electroweak matter.

At the saddle point of the integral, $\zeta'-\zeta\approx 3/D$, corresponding to the ratio of the bubble radius to the horizon

$$v(t-t')/2t\approx 3v/(2D_\chi)\approx 4\times 10^{-5}v\ .$$

So when the bubbles collide and fill space, they are very much smaller than the horizon, but very much larger than the correlation length $m_H(T)^{-1}\approx 10T^{-1}\approx 10^{-15}t$. During the growth of these bubbles, the temperature of the Universe decreases due to the expansion of the Universe by approximately $4\times 10^{-5}$, a negligible effect. Such bubbles do generate density fluctuations, but of quite small amplitude $\sim 10^{-4}$, and on a mass scale of order $10^{12}$ kg—roughly the mass of a small mountain! The density fluctuations are not likely to be large enough to significantly affect nucleosynthesis.

## III. PROPAGATION OF THE NUCLEATION BUBBLES

The theory of phase-transition bubbles expanding into a thermal plasma has been studied in Refs. [26,27]. In that analysis, it was assumed that the phase-transition bubble propagates without generation of hydrodynamic instability. In many types of phase transitions, the growth of nucleation bubbles may be unstable, and the proper solution to the problem does not involve bubbles with well-defined surfaces. This problem certainly deserves attention in the context of the electroweak phase transition, and has been addressed somewhat for the *QCD* phase transition [30]. In this paper, we will assume propagation of stable bubble walls, and leave the problem of understanding the various types of instabilities which might develop for later work.

Assuming stable propagating bubbles, there are two types of solutions, called deflagrations and detonations. As the names suggest, deflagrations correspond to slow burning, and detonations to rapid burning.

These bubbles are best analyzed using local energy density, as measured in the rest frame of the fluid, and the local rapidity of the fluid

$$\Theta=\frac{1}{2}\ln\left[\frac{1+v}{1-v}\right] \tag{27}$$

and the space-time rapidity

$$y=\frac{1}{2}\ln\left[\frac{t+x}{t-x}\right]\ . \tag{28}$$

We assume the bubble starts at $t=x=0$. The fact that the solution depends only on the ratio of $t/x$ is a well-known scaling property of hydrodynamic equations, and is applicable when the bubble is large compared to a mi-

croscopic distance scale.

The typical bubble configuration for a deflagration is shown in Fig. 2. On the far left in this figure, the matter is at rest and is in the broken-symmetry phase. There is a discontinuity in the flow velocity and energy density of the fluid when the matter is converted from symmetric to asymmetric matter. The energy released due to the latent heat of the phase transition is converted into motion of the fluid in front of the surface of discontinuity. This fluid propagates with a uniform velocity until a second supersonic shock-wave discontinuity is encountered. On both sides of the shock front the matter is in the symmetric phase. The matter is compressed and accelerated by the shock front. To the right of the shock front, the fluid is at rest.

A typical detonation bubble is shown in Fig. 3. To the right of the fluid the system is at rest. There is a discontinuity which corresponds to the phase transition as we move in from the right. To the left of the surface of discontinuity, there is a similarity rarefraction wave where the matter slows down and is rarefied. At the position $y_s$, the energy density and velocity are continuous, but there is a discontinuity in the first derivative of the velocity.

From the figures, it is obvious what is happening physically. In a deflagration, the velocity of the deflagration front is sufficiently slow so that the matter distribution in front of the phase-transition region may be compressed and accelerated. For a detonation, the region of the phase transition propagates so rapidly that there is no time for the fluid in front of the shock to be accelerated. It is similar to the difference between a supersonic and subsonic perturbation in a fluid.

The mathematical criterion which distinguishes a deflagration from a detonation may be analyzed in the rest frame of the phase boundary. We show a picture of the phase boundary in Fig. 4. For a deflagration, the velocity of the fluid to the right, $v_2$, is less than that to the left, $v_2 \leq v_1$. For a detonation the opposite is the case, $v_2 \geq v_1$.

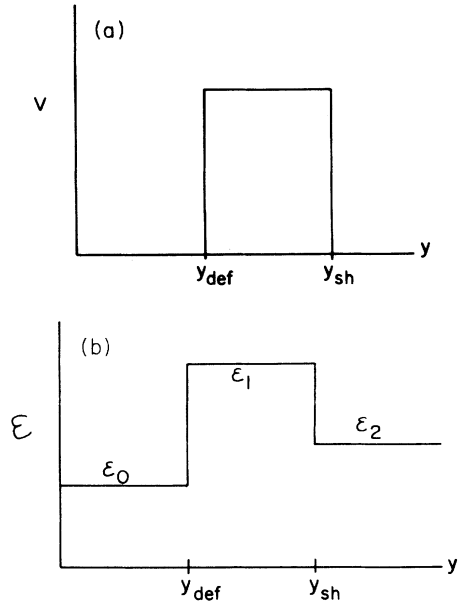


FIG. 2. (a) The flow velocities of the matter distribution for a deflagration bubble. (b) The local energy densities for a deflagration bubble.

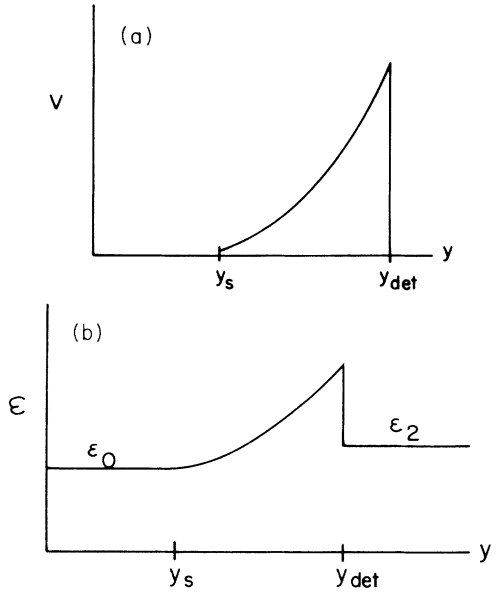


FIG. 3. (a) The flow velocities of the matter distribution for a detonation bubble. (b) The local energy densities for a detonation bubble.

The velocities and energy densities in the cases of a deflagration and a detonation front are determined entirely by energy and momentum conservation and by the amount of entropy production across the surfaces of discontinuity. In the rest frame of the surface of discontinuity, we have constant energy flux and momentum flux,

$$\partial_x T^{xt} = \partial_x T^{xx} = 0 \tag{29}$$

and

$$\partial_x s^x \geq 0 \tag{30}$$

where we use the perfect-fluid form for the stress-energy tensor

$$T^{\mu\nu} = (\epsilon + P) u^\mu u^\nu - P g^{\mu\nu} \tag{31}$$

so (29) becomes

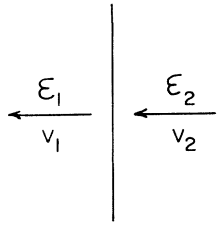


FIG. 4. The flame front in the rest frame of the front.

$$T^{xt}=(\epsilon+P)\gamma_v^2 v=\text{const}\ ,$$
$$T^{xx}=(\epsilon+P)(\gamma_v v)^2+P=\text{const}\ , \tag{32}$$

and

$$s^\mu=su^\mu \tag{33}$$

where $s$ is the entropy density in the rest frame of the fluid. The four-velocity of the fluid is $u^\mu$ and satisfies $u^2=-1$. If the number of particles is conserved, we should have another equation

$$\partial_x n^x=0 \rightarrow n\gamma v=\text{const} \tag{34}$$

where $n^\mu$ is the number current, given by

$$n^\mu=nu^\mu\ , \tag{35}$$

and $n$ is the number density in the rest frame of the fluid.

The local energy density is $\epsilon$, the pressure is $P$, and the entropy density is $s$. Integrating (29) across the discontinuity gives for the velocities of the fluid

$$v_1^2=\frac{(P_1-P_2)(\epsilon_2+P_1)}{(\epsilon_1-\epsilon_2)(\epsilon_1+P_2)} \tag{36}$$

and

$$v_2^2=\frac{(P_1-P_2)(\epsilon_1+P_2)}{(\epsilon_1-\epsilon_2)(\epsilon_2+P_1)}\ . \tag{37}$$

If we boost to the frame where $v_1=0$, we find the velocity of the fluid on the right of the front to be

$$v_{\text{ret}}=\left[\frac{(P_1-P_2)(\epsilon_1-\epsilon_2)}{(\epsilon_1+P_2)(\epsilon_2+P_1)}\right]^{1/2}\ . \tag{38}$$

These equations are not sufficient to determine the energy densities and velocities. If particle number is not conserved, we have three unknowns: the temperature and velocity of the fluid behind the phase boundary, and the velocity of the phase boundary. But we only have two equations (29). Likewise, if particle number *is* conserved, we have an extra equation, (34), but also an extra unknown: the chemical potential behind the phase boundary. Another equation is needed in order to determine the velocity of the phase boundary, which will then fix everything. This extra equation may be taken to be the equation of motion of the Higgs field [25], and its solution will, as we shall see, depend strongly on the details of the microscopic physics. It will be the objective of subsequent sections to derive an equation for the motion of the bubble wall.

## IV. THE EQUATION WHICH DETERMINES THE VELOCITY OF BURNING

In the preceding section, we saw that the hydrodynamic equations alone are not sufficient to determine the velocity of the phase boundary. To do this, we must understand the microscopic dynamics governing the motion of the Higgs field.

Before proceeding with this, we first observe that the change in the temperature across the burning front is negligible. This is because the latent heat of the transition is very much smaller than the specific heat of the plasma. The only effect of the phase transition is to give small masses to a few of the particles. For all of the quarks except the top quark, the mass is very small. For the Higgs boson, the generated mass should also be small, and for the $W$- and $Z$-boson mass it is of order $T/3$, which is small compared to the average kinetic energy, which is about $3T$. Gluons and photons remain massless. When explicitly computed [25], the resulting temperature change is very small; $\delta T \ll 1$. In this circumstance, it will be a good approximation to neglect the change in temperature for the fluid as a whole across the phase-transition boundary (although as we shall see, there is an effective temperature change in the distribution of $W$ bosons alone which is important).

For similar reasons, the change in the velocity of the fluid across the wall is very small—the medium has very large inertia, and the force is small. To leading order, it is a good approximation to ignore the change in fluid velocity across the bubble wall when computing the effective equation for the Higgs field. Once the velocity of the bubble wall is known, one can use the equations of the preceding section to determine whether the phase boundary is a detonation or a deflagration. Roughly speaking, if the phase boundary moves faster than $1/\sqrt{3}$ times the speed of sound then it is a detonation. If it moves slower than the speed of sound it is a deflagration.

The dynamical equation which determines the motion of the bubble wall is the scalar field equation. To first nonzero order in the loop expansion, the scalar field equation is

$$-\partial^2\phi(x)+\frac{\delta V}{\delta\phi}(x)+\int d^4x'\Sigma(x,x')\phi(x')=0\ . \tag{39}$$

The one-loop Feynman diagrams for $\Sigma$ are shown in Fig. 5. These include contributions from the Higgs bosons, the $W$ and $Z$ bosons, and from quarks and leptons. In the diagram, the propagators are taken to be at finite temperature in the presence of the external scalar field which forms the phase boundary. For the gauge bosons getting their mass from the Higgs field, for example, $\Sigma$ may be thought of as the average of the square of the

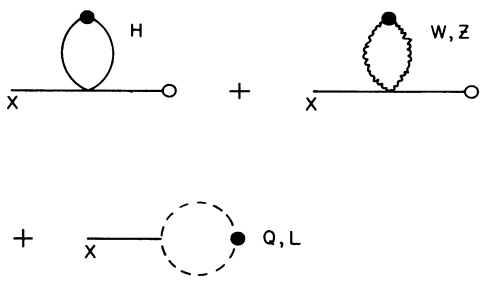


FIG. 5. The contributions to the self energy kernel for the scalar field equation. All propagators are in the background fields associated with the phase transition boundary. (a) The contribution of Higgs particles. (b) The contribution of the $W$ and $Z$ bosons. (c) The contribution of quarks and leptons.

gauge fields, the average being taken in the appropriate thermal state.

Needless to say, the solution of this equation is very hard due to the dependence of the loop diagrams on the external field. However, if we expand the loop diagrams in powers of the external field, the equation simplifies. This expansion should be reasonable when the temperature is large compared to the mass. In particular, it should be excellent for all quarks and leptons except perhaps for the top quark, and for the Higgs boson.

The leading-order contributions to $\Sigma$ when $M/T \ll 1$ are shown in Fig. 6. These diagrams have been written as phase-space integrals over the finite-temperature distribution functions

$$f(p,x)=\frac{1}{e^{\beta\gamma(E-vP_x)}\mp 1} \tag{40}$$

where the plus sign is for fermions and the minus sign is for bosons. The integration is a three-dimensional integral taken on mass shell for the lines which have been cut in Fig. 6. The factors of $\gamma$ and of $v$ refer to the velocity of the electroweak fluid, which we allow to be moving.

The integration for $\Sigma$ in the Feynman diagram of Fig. 6 has measure $d^3P/E$ which is Lorentz invariant, so that even if the electroweak fluid is moving, to leading order there is no dependence on the velocity of the fluid. Therefore, to leading order in the mass expansion, the result for $\Sigma$ is just the finite-temperature modification of the scalar-particle mass. This converts the derivative of the scalar potential in the above equation almost into the derivative of the finite-temperature effective potential.

The terms in the scalar field equation arising at one-loop order combined together with the derivative of the scalar potential would be precisely the derivative of the three-dimensional effective potential if we also included one higher-order term in the mass when expanding the loop diagram. This would naively generate the contribution to the effective potential, which is of order $\phi^3 T$. Higher-order terms in the expansion of loops in this effective mass could be ignored if the coupling constant were small, since such contributions contain no factors of $T$.

For the moment we therefore concentrate on the contribution which is of order $\phi^3 T$. This term arises only from the contribution of the boson loops. The fermion-loop contribution therefore only contributes to a mass renormalization as long as an expansion in $M/T$ is sensible. This will be the case for all fermions except for the top quark. We will here assume that the top quark is of sufficiently small mass that this is true, but in reality a good computation should include this contribution, and should as well include contributions of order $\phi^3 T$ arising from higher-order terms in the loop expansion. This has been done by Carrington [15–34], but we shall not consider these effects further here. In the last section of this paper, when we consider wall motion in the limit that the scattering length is small compared to the size of the phase-transition bubble wall, we shall attempt to estimate the effect of top quarks to the damping of the bubble-wall motion.

In these approximations, the only important contributions arise from boson loops. Assuming that the Higgs-boson mass is small compared to that of the $Z$ and $W$ bosons, $M_H(T) \ll M_W(t)$, we can as well ignore the contribution from Higgs bosons. The only contribution therefore arises from $W$- and $Z$-boson loops.

To leading order in the mass expansion, the dominant contribution is given by the tadpole diagram of Fig. 7. This contribution would also be of order $\phi^4$, if it were not for the infrared singularity associated with the Bose-Einstein distribution function. However, if we compute this contribution by expanding, we find a result which is not independent of $\gamma$ and $v$, so that we must be careful about the electroweak fluid velocity. This is particularly important when the electroweak fluid has a different velocity on either side of the wall. In the next section, we describe how to properly compute for this case. Notice also that the formal expansion in the external field generates a loop contribution for the scalar field equation with a nonzero imaginary part corresponding to Landau damping.

For the rest of this section, we shall describe the solution to the scalar field equation when we assume that the loop corrections only transform the scalar potential into the finite-temperature effective potential. In this case, for $\zeta \leq 2$, the bubble will accelerate indefinitely, with the bub-

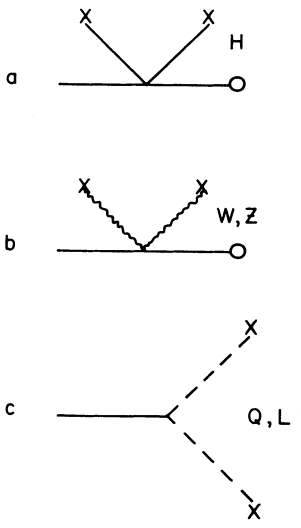


FIG. 6. The leading contributions of $\Sigma$ when the mass is much less than the temperature. (a) The contribution of Higgs particles. (b) The contribution of $W$ and $Z$ bosons. (c) The contribution of quarks and leptons.

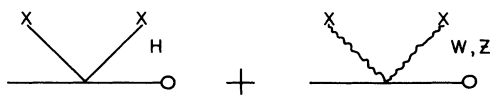


FIG. 7. The tadpole contribution to the scalar self energy kernel $\Sigma$.

ble wall approaching the speed of light. This follows because the energy released from undergoing the phase transition must go into the acceleration of the bubble wall.

The effect of damping is therefore to make the wall acquire some finite velocity. We therefore expect that when the damping effects are properly included, the solution of the scalar field equation will take the form

$$\phi=\phi(\gamma(x-vt)) . \tag{41}$$

For the classical equation without damping, we can see that such a solution which interpolates at large distance between the local minima of the effective potential is not possible. The equation

$$-\partial^2\phi(\gamma(x-vt))+\frac{\delta V}{\delta\phi}(x)=0 \tag{42}$$

becomes

$$-\frac{d^2}{d\tau^2}\phi(\tau)+\frac{\delta V}{\delta\phi}(\tau)=0 , \tag{43}$$

where $\tau=\gamma(x-vt)$. This equation describes a particle rolling in an inverted potential $-V$. If the potential is inverted, the only allowable solutions which are nonsingular at infinite $\tau$ are bounce solutions or trivial solutions. There is no solution where the field is in one minimum at large positive $\tau$ and in the other minimum at large negative $\tau$.

When damping is included, such solutions become possible. For example if the equation becomes

$$\frac{d^2}{dt^2}\phi+\eta\frac{d}{dt}\phi-\frac{d}{dx^2}\phi+\frac{\delta V}{\delta\phi}=0 \tag{44}$$

the ansatz (41) leads to an equation for a particle with damping coefficient $\eta\gamma v$. It is then clear from a standard "undershoot-overshoot" argument that an appropriate value of the damping coefficient exists such that the particle begins at the true vacuum at minus infinite $\tau$ and rolls to the false vacuum at plus infinite $\tau$. This value determines the final velocity of propagation of the bubble wall. In fact, by multiplying the equation by $d\phi/d\tau$ and integrating, one obtains

$$\eta\gamma v\int d\tau(d\phi/d\tau)^2=\Delta V \tag{45}$$

with $\Delta V$ the potential-energy difference between the two vacua. This is a sort of virial theorem—the left-hand side represents the rate of loss of energy per unit distance the wall propagates, per unit area, due to the damping term, and the right-hand side the energy density difference between the false and true vacua. This kind of argument will be useful when more general damping forces are included.

In the preceding section, we argued that the parameter $\zeta$ which characterizes the effective potential is about $\zeta\sim1.6$ which is close to the value of $\zeta=2$ where the effective potential is degenerate at the two minima. In this case, we expect that when damping is included, the deviations away from the limiting case of $\zeta=2$ should be small. The left-hand side of (45) would then be calculated using the bubble-wall solution which holds at $\zeta=2$, and would determine the velocity $v$. The solution takes the approximate form (41) with $\phi$ the static domain-wall solution. The main effect should be to narrow the apparent thickness of the wall by a factor of $1/\gamma$ and have it move with velocity $v$.

In the case when $\zeta=2$, the solution for the static domain wall is a kink. The dimensionless effective potential is then

$$V(x,\zeta=2)=\tfrac{1}{4}g^2(g-2)^2 \tag{46}$$

with the kink solution being given by

$$g=1+\tanh\left[\frac{x}{\sqrt{2}}\right] \tag{47}$$

$$=1+\tanh\left[\left[\frac{1}{2\lambda}\right]^{1/2}\delta Tr\right] \tag{48}$$

where we have reexpressed the result originally in terms of the dimensionless variable $x$ in terms of the physical coordinate $r$.

The width of the wall is $\sim 2m_H(T)^{-1}$

$$L\sim\frac{\sqrt{2\lambda}}{\delta T} \tag{49}$$

$$\sim\frac{4}{3\alpha_W}\frac{M_H}{M_W}\frac{1}{T} \tag{50}$$

$$\sim(15-25)T^{-1} , \tag{51}$$

where in the last equation we used the bounds on the Higgs mass discussed in the introduction. The width of the bubble wall is therefore of the order of $L\leq 20/T$ and is typically very large compared to a thermal wavelength or a $W$- or $Z$-boson mass near the transition. When the bubble-wall motion is accounted for, the width shrinks a little by a factor of $1/\gamma$, but for mildly relativistic motion this is not a big effect. The limit appropriate for describing the bubble dynamics is therefore that of a thick bubble wall, not a thin one. In this case, the WKB approximation is good, and particle scattering off the wall is well described by the classical limit, the bubble wall being either reflectionless or transmissionless depending on the particle kinetic energy.

It is useful to compare the size of the bubble wall to an estimate of the mean free path for the particles which scatter off the wall. The dominant contribution to the damping term must come from $W$ and $Z$ boson loops as was argued above. This is true because fermions have small masses except for the top quark, and the top-quark contribution for intermediate values of the top-quark mass will only effect the finite temperature contribution to the scalar boson mass. The Higgs boson contribution is small since the Higgs mass is small. We therefore must discuss the degree of thermalization of $W$ and $Z$ bosons.

The mean free path for a $W$ or $Z$ boson is of order

$$\lambda_{\rm mfp}\sim\frac{1}{\sigma n} \tag{52}$$

where $\sigma$ is the cross section for scattering and $n$ is the density of particles off of which the $W$ and $Z$ bosons scatter. Since we are interested in effects generated by the bubble wall, and this effects primarily particles with energy of order $M_W$, we expect that the cross section should be of order

$$\sigma \sim 2\pi \frac{\alpha_W^2}{M_W^2(T)} . \tag{53}$$

To derive this formula, we have assumed that Coulomb scattering is dominant at momentum transfers of order $M_W$. We expect that Coulomb scattering will dominate the cross section at small momentum transfers.

The density is given by the density per species times the number of species $N$. The factor $N$ is the number of particles participating in the Coulomb scattering. Remembering that for each fermion there is only one helicity which participates in the weak interactions, particle and antiparticle, two doublets, three families, and a quark and lepton which can scatter weakly, the factor $N$ is

$$N = 48 \tag{54}$$

for fermions alone. There is an additional contribution for $W$, $Z$, and Higgs bosons which corrects this by about 20%, which is small because of the small number of such particles compared to the number of fermions. The number density per fermion is on the other hand about $T^3/\pi^2$, so that we have approximately

$$n \sim 5T^3 . \tag{55}$$

The mean free path is therefore about

$$\lambda_{\rm mfp} \sim \frac{M_W^2}{10\pi\alpha_W^2 T^3} . \tag{56}$$

Using $M_W \sim T/4 - T/2$, we have

$$\lambda_{\rm mfp} \sim (2-8)T^{-1} . \tag{57}$$

This estimate gives a mean free path which is not very much less than the width of the bubble wall. We expect therefore that the effects of deviation from equilibrium will be of order 1 and must be carefully estimated.

It should also be noted that in models where scattering from a bubble wall is responsible for generating a baryon asymmetry, the effect must arise because of a difference in the reflection coefficients for top quark and antiquark. This can only happen if there are nontrivial values of both reflection and transmission coefficients and therefore the momentum of the top quark must be of order $M_t$. In this region, as we previously noted, the WKB approximation should be good, so that the deviations from triviality must arise from exponentially suppressed contributions of order $e^{-M_t L} \sim e^{-20}$, where $L$ is the size of the phase-transition bubble wall. This exponential suppression can be to some degree ameliorated by requiring that the momentum of the top quark be tuned so that when the quark passes over the bubble wall, its momentum is very small so that it effectively sees a thin wall. This puts a strong constraint on the phase space, and leads to suppressions by powers of $1/LM_t$. Moreover, the mean free path for Coulomb scattering of such a low-momentum quark is much smaller than that estimated in Eq. (57), being determined by strong scattering, with cross section $\sim \pi\alpha_S^2/M_t^2$. This yields $\lambda \sim 0.4/T \ll L$. Both of these conclusions contradict the assumptions made in Refs. [22,23].

## V. BUBBLE-WALL DAMPING IN THE LIMIT $\lambda_{\rm mfp} \geq L$

In the limit that the particle mean free path is large compared to the thickness of the bubble wall, the calculation simplifies greatly. We will later study the limit where the mean free path is small compared to the wall size, and find that this is the more relevant limit. The computation here is, however, sufficiently simple and is related directly to previous attempts to compute the bubble-wall velocity. It also illuminates the approximations needed to compute in the more realistic small-mean-free-path case.

To solve this problem, we will work in the rest frame of the bubble wall. In this frame, the electroweak fluid is moving, and the scalar field is a function only of its spatial coordinate $\mathbf{x}$. The profile of a bubble wall is as shown in Fig. 8, and in the frame where the fluid would be at rest, the bubble wall would be moving to the left.

As discussed above, we will consider the contribution to the scalar field equation arising from loops with only $W$ and $Z$ bosons. The contributions of fermions and Higgs bosons will be taken only as that which gives a finite-temperature redefinition of the scalar-particle mass. Finally, we will assume that the wall perturbs the system only slightly. We will therefore assume that to leading order in the computation of the wall velocity, the fluid on either side of the phase-transition bubble wall has the same temperature and the same velocity.

The contribution of the $W$ and $Z$ bosons to the scalar field equation of motion is given by the Feynman diagram shown in Fig. 7. This contribution is local in coordinate space and may be written as

$$\rho(x) = \tfrac{1}{2} g^2 \phi(x) \eta(x) , \tag{58}$$

where

$$\eta(x) = \sum_N \langle a_N^\dagger(\mathbf{x}) a_N(\mathbf{x}) \rangle . \tag{59}$$

In this equation, the sum over $N$ is a sum over all energy eigenstates in the field generated by the scalar potential $\phi$. The brackets mean to weight the sum with some statistical ensemble which corresponds to the temperature and velocity of the fluid. Notice that because of the dependence of the sum on the scalar field $\phi$, this equation introduces nonlinearity in the evaluation of $\phi$ from its equation of motion, and the problem of computing the sum for arbitrary $\phi$ is incredibly difficult.

In the statistical matrix, we assume a weight function given by

$$f(p,x) = \frac{1}{e^{\beta\gamma(E_N - vP_N^z)} - 1} \tag{60}$$

where we have chosen the bubble wall to be along the $z$ axis. This would be the sum we would choose for a moving fluid. The index $N$ refers to the $N$th energy eigenstate of the scalar field in the presence of the wall.

Of course the sum as it stands does not make sense, since in the presence of the external field $\phi(\mathbf{x})$, the solutions for the $W$ and $Z$ wave functions are not eigenstates of $P^z$. This results in two different problems. For the geometry of Fig. 8, there are two types of waves which are right moving. There are those with a momentum insufficient to go across the domain wall, and there are those with sufficient moment. For those with insufficient momentum, the solution for the $W$ and $Z$ equations of motion is a sum of a left-moving and a right-moving wave. We interpret this as a right-moving wave plus a reflected left-moving wave. We identify the momentum as that of the right-moving wave measured far to the left of the bubble wall. For waves with sufficient momentum to cross the barrier, we also identify the spatial momenta of such right-moving waves as that measured far to the left of the wall. For the left-moving wave, which originally come from the far right of the wall, we measure the momentum as that of the left-moving wave measured far to the right of the wall. These identifications of the wave momenta are consistent with a picture where the right-moving waves arise from a heat bath far to the left of the wall, and the left-moving waves from a heat bath far to the right of the wall. These heat baths far to the right and left are assumed to have the same temperature and velocity. Notice that here we are making a crucial assumption that the length scale for thermalization, that is, particle mean free paths, are large compared to the bubble size.

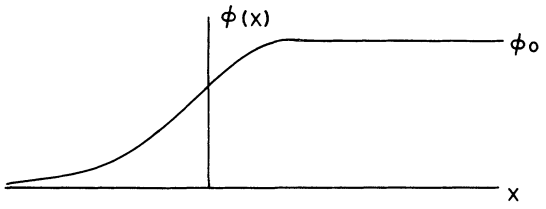


FIG. 8. The profile of the bubble wall, in its rest frame, with the fluid flowing to the right.

With this identification of the momenta, the sum for $\eta$ becomes

$$\eta(\mathbf{x})=\sum_N \left[ \frac{\theta(p_N^z)}{e^{\beta\gamma(E_N-v\sqrt{E_N^2-p_t^2})}-1}+\frac{\theta(-p_N^z)}{e^{\beta\gamma(E_N+v\sqrt{E_N^2-p_t^2-M^2})}-1} \right] \psi_N^\dagger(\mathbf{x})\psi_N(\mathbf{x}) \tag{61}$$

where we are now using $M_Z=M$. In this equation, the wave function for the $W$ and $Z$ field in the presence of the background scalar field is denoted by $\psi$. We have chosen to label our states by energy and by transverse momentum $p_t$. For the states with positive $p_z$, we require that $E_N \geq |p_t|$, and for negative $p^z$ that $E_N \geq \sqrt{p_t^2+M^2}$.

The previous equation as it stands would be very difficult to evaluate, since there is an implicit dependence in the wave functions on the scalar field $\phi$. However, it can be evaluated in the WKB approximation. This approximation assumes that the scale size of spatial variation of the wall is large compared to the scale of variation of the wave function. The relevant momenta are $k \sim M$, and the size of the bubble wall is $L \sim 1/\alpha_W T$. This requires that $M \gg \alpha_W T$, a condition which appears to be satisfied.

We can now determine the wave functions. For $0 \leq p^z \leq M$, the WKB wave functions are standing waves. Defining $E_\parallel=\sqrt{E_N^2-p_t^2}$, we have

$$\psi_N(\mathbf{x})=\left[\frac{4E_\parallel}{L_z}\right]^{1/2}\frac{1}{\sqrt{q(z)}}e^{ip_t\cdot x_t}\cos\left[\int_{z_0}^z dz' q(z')-\pi/4\right] . \tag{62}$$

In this equation, the space-dependent WKB momentum is

$$q(z)=\sqrt{E_\parallel^2-M^2(z)} . \tag{63}$$

The parameter $L_z$ is a length along the $z$ axis in which we choose to quantize the system. It is necessary for counting states, but will drop out in the end of our computations. The value of $z_0$ is the $z$ coordinate where the WKB momentum vanishes; that is the turning point for the reflected wave. The WKB quantization condition is here

$$E_\parallel=\frac{2\pi N}{L_z} . \tag{64}$$

For the case where the $W$- and $Z$-boson fields have energy sufficient not to be reflected by the barrier, there are two solutions corresponding to left- and right-moving waves. There are

$$\psi_N(\mathbf{x})=\left[\frac{2E_\parallel\sqrt{E_\parallel^2-M^2}}{L_z(E_\parallel+\sqrt{E_\parallel^2-M^2})}\right]^{1/2}\frac{1}{\sqrt{q(z)}}e^{ip_t\cdot x_t}\exp\left[\pm i\int_{-\infty}^z dz' q(z')\right] . \tag{65}$$

In this equation all quantities are as defined for the reflected wave. The WKB quantization condition is here

$$\frac{1}{2}(E_{\parallel}^2+\sqrt{E_{\parallel}^2-M^2})=\frac{2\pi N}{L} . \tag{66}$$

We can now insert these expressions for the wave function into the expression for $\eta(x)$. In doing this the reflected-wave term squares to an average value plus a rapidly oscillating value. We ignore the contribution which is rapidly oscillating as this will average to zero in the sum over states. After some algebra, the sum over states may be written as

$$\eta(\mathbf{x})=\frac{1}{2}\int\frac{d^3k}{(2\pi)^3}\theta(k_z-M)\frac{k_z}{|\mathbf{k}|}\frac{1}{\sqrt{k_z^2-M^2(z)}}\frac{1}{e^{\beta\gamma(|\mathbf{k}|-vk_z)}-1}$$
$$+\theta(M-k_z)\theta(k_z-M(z))\frac{2k_z}{|\mathbf{k}|}\frac{1}{\sqrt{k_z^2-M^2(z)}}\frac{1}{e^{\beta\gamma(|\mathbf{k}|-vk_z)}-1}+\theta(-k_z)\frac{1}{\sqrt{k_z^2+M^2}}\frac{k_z}{\sqrt{ks_z^2+M^2-M^2(z)}} . \tag{67}$$

We can understand this WKB evaluation in a simple way. We observe that the contribution of the tadpole term to the equation of motion is

$$\rho(x)=\tfrac{1}{2}g^2\phi(x)\eta(x) \tag{68}$$
$$=\frac{dM^2(x)}{d\phi(x)}\eta(x) . \tag{69}$$

To determine the contribution of this term to the equations of motion, we can integrate with respect to $\phi(x)$. In doing this, we will be interested in the potential difference between different sides of the bubble wall. We will get a stable solution when the velocity-dependent effects allow for a degenerate value of the potential far from the bubble wall. We therefore need only integrate for $0\le M(z)\le M$. Integrating with respect to $\phi(x)$ to determine the tadpole diagram's contribution to the equation of motion,

$$V_{\rm tad}=\frac{1}{2}\int\frac{d^3k}{(2\pi)^3}\theta(k_z-M)\frac{k_z}{|\mathbf{k}|}(k_z-\sqrt{k_z^2-M^2})\frac{1}{e^{\beta\gamma(|\mathbf{k}|-vk_z)}-1}$$
$$+\theta(M-k_z)\theta(k_z)\frac{2k_z}{|\mathbf{k}|}k_z\frac{1}{e^{\beta\gamma(|\mathbf{k}|-vk_z)}-1}+\theta(-k_z)\frac{k_z}{\sqrt{k_z^2+M^2}}(\sqrt{k_z^2+M^2}-k_z) . \tag{70}$$

This expression can be rewritten as the sum of two terms,

$$V_{\rm tad}=P_R+P_L , \tag{71}$$

where

$$P_R=\int\frac{d^3k}{(2\pi)^3}\frac{1}{e^{\beta\gamma(|\mathbf{k}|-vk_z)}-1} \tag{72}$$
$$\times\frac{k_z}{|\mathbf{k}|}[\theta(k_z-M)(k_z-\sqrt{k_z^2-M^2})+\theta(M-k_z)\theta(k_z)2k_z] \tag{73}$$

and

$$P_L=\int\frac{d^3k}{(2\pi)^3}\frac{1}{e^{\beta\gamma(E_k+vk_z)}}\frac{k_z}{E_k}\theta(k_z)(\sqrt{k_z^2+M^2}-k_z) . \tag{74}$$

We can easily interpret this result. The first term $P_R$ is the pressure arising from right-moving particles coming from the left. The factor of $k_z/|\mathbf{k}|$ is the flux factor of particles from the left. The factor in brackets is the change in momentum for particles with momentum large enough to pass over the bubble wall (first factor), and for those with insufficient momentum which are reflected from the wall (second factor). The term $P_L$ is the pressure from left-moving particles coming from the right of the bubble wall.

It is now straightforward to perform these integrations to obtain an effective potential. The result for small $v$ is computed to be

$$V_{\rm tad}=\frac{M^2T^2}{24}-\frac{M^3T}{12\pi}\left[1-\frac{3v}{\pi}\right] . \tag{75}$$

The total contribution to the effective potential comes from summing over spin and charge states of the $W$ and $Z$ bosons, which gives an overall factor of 9.

The change in the thermodynamic potential due to the tadpole term generates the quadratic and cubic terms in the finite-temperature effective potential, up to a correction which is

$$\Delta V=-3\frac{\delta v}{\pi}T\phi^3 . \tag{76}$$

The main effect is to rescale the parameter $\delta$ by a velocity-dependent term. This will increase the effective value of $\zeta$, $\zeta_{\rm eff}=\zeta/(1-3v/\pi)^2$. The wall will cease to be accelerated when degeneracy of the two vacua occurs—i.e., when $\zeta_{\rm eff}=2$, or

$$v=\frac{\pi}{3}(1-\sqrt{\zeta/2}) . \tag{77}$$

For the value appropriate for bubble nucleation, $\zeta=1.6$ so that

$$v\sim 0.1 . \tag{78}$$

We should note that this estimate assumes maximum deviation from thermal equilibrium—we have used the unperturbed distribution functions far to the left and the right of the wall. This is reasonable only if the mean free path for particle scattering is assumed large compared to the size of the bubble wall. On the other hand, in the fully equilibrated limit, the analysis above and that in Ref. [25] show that the bubble wall is not stopped. Therefore, the above estimate provides a *lower bound* on the velocity of the bubble wall. In the next section, we assume that the distribution of particles is actually quite close to equilibrium, and will compute it in an expansion in the mean free path divided by the size of the bubble wall.

## VI. THE WALL VELOCITY WHEN $\lambda_{\rm mfp}/L \ll 1$

We now want to compute the effect of the tadpole term on the scalar field equation of motion in the more realistic limit where the deviation from equilibrium is small. Recall that the function $\eta(x)$ for each particle species may be written as

$$\eta(x)=\int\frac{d^3p}{(2\pi)^3 2E}f(p,x) , \tag{79}$$

where $f(p,x)$ is the single-particle Wigner distribution function. This may be proven formally by using the definition of the single-particle Wigner distribution function, by taking the expectation value $\langle\phi^2\rangle$ for a free field. It includes the WKB result which we discussed above as a special case. This result may also be derived using real-time response theory and relativistic kinetic theory [32].

As discussed above, we expect that the most significant deviation from local thermal equilibrium arises from $W$ and $Z$ bosons. The only possible large fermion contribution comes from the top quark. As we discussed above, this contribution must be treated specially for large top-quark masses, but for small top-quark mass has no infrared-singular part and is expected only to add a finite temperature correction to the scalar mass. In addition, if the deviations from equilibrium are small, the top quark due to its strong interactions should be closer to equilibrium than the $W$ and $Z$ bosons. The Higgs boson may be ignored since the small Higgs mass implies only a small coupling through the tadpole in the scalar field equation.

The single-particle distribution functions satisfy the Uehling-Uhlenbeck (Boltzmann) equation of relativistic kinetic theory [32]. For a boson distribution function $f(x,p)$, this equation is

$$[p\cdot\partial_x+M(x)F\cdot\partial_p]f(p,x)=C(x,p) . \tag{80}$$

In this equation, $F^\mu$ is a covariant force term, and $C(p,x)$ is a collision integral which will be discussed below. All dot products are over covariant four vectors. Notice that if we think of the distribution function as only a function of $\mathbf{p}$, then only spatial derivatives with respect to momentum appear. The above equation may be derived assuming the constancy of particle number flux through a timelike three-surface.

The force on each particle is found from energy conservation in the wall rest frame

$$\mathbf{k}^2+M(x)^2=\text{const} \tag{81}$$

so that the spatial component of the four-force $\mathbf{F}=d\mathbf{k}/d\tau$ is given by

$$\mathbf{F}=-\frac{1}{2M(x)}\nabla M^2(x) . \tag{82}$$

In the limit where the mean free path for collisions is small, the collision term in the Boltzmann equation forces the distribution functions to take the local thermal equilibrium form:

$$f_{\rm eq}(p,x)=\frac{1}{e^{\beta(x)[\gamma_v(E-v(x)p_x)-\mu(x)]}-1} , \tag{83}$$

where the temperature $\beta$, the fluid velocity $v$ and (in the case where particle number is conserved) the chemical potential may depend on $x$. It is straightforward to compute the net pressure exerted on the wall by particles in this distribution colliding with the wall, by integrating the number density of particles across the wall multiplied by the force the wall applies on them [the relevant force in the wall frame is $\mathbf{F}=d\mathbf{k}/dt=-(1/2E)dM^2/dx$]:

$$P_{\rm coll}=\int_{-\infty}^{\infty}dx\frac{dM^2(x)}{dx}\int\frac{d^3k}{(2\pi)^3}\frac{1}{2E}\frac{1}{e^{\beta(x)[\gamma(E-v(x)k_x)-\mu(x)]}-1} \tag{84}$$

for bosons, and similarly for fermions. Changing variables to $k_x'=\gamma_v(k_x-v(x)E)$ one finds that the velocity dependence completely disappears. While the apparent number density of particles in the rest frame of the wall rises (due to Lorentz contraction), they have higher energy, and the wall is more transparent to them. These opposing effects exactly cancel [25].

In the regime of interest, where $\lambda_{\rm mfp}/L \ll 1$, we expect the phase-space density to remain close to the above local equilibrium form. The general procedure for solving the

transport equation in this case is as follows. As the zeroth-order solution, we take the limit when the mean free path goes to zero, and the collision term forces the distribution function into the local equilibrium form. The temperature, velocity, and chemical potential (nonzero only if particle number is conserved) are allowed to depend on $x$. However, the three equations of energy, momentum, and particle-number conservation discussed above, (32) and (34), are enough to completely fix these as a function of $M^2$, and therefore of $x$. We then expand the distribution function around the local equilibrium solution

$$f(p,x)=f_{\rm eq}(p,x)+\delta f(p,x) \tag{85}$$

while imposing the following conditions on $\delta f(p,x)$:

$$\delta T^{xx}=\frac{1}{(2\pi)^3}\int\frac{d^3p}{E}\delta f(p,x)k^x k^x=0\ , \tag{86}$$

$$\delta T^{xt}=\frac{1}{(2\pi)^3}\int\frac{d^3p}{E}\delta f(p,x)k^x E=0\ , \tag{87}$$

$$\delta n^x=\frac{1}{(2\pi)^3}\int\frac{d^3p}{E}\delta f(p,x)k^x=0\ , \tag{88}$$

which are necessary in order to ensure that the perturbation still obeys the conservation laws. These equations are also just enough to uniquely determine the solution to the transport equation—they eliminate perturbations corresponding simply to a shift in the temperature, velocity, or chemical potential of the fluid as a whole.

Now if we substitute (85) into the transport equation, the lowest-order equilibrium distribution functions make the collision term vanish. The collision term is therefore only nonzero beginning with the first-order deviations from the thermal equilibrium distribution functions. On the other hand, the left-hand side of this equation generates derivatives on the lowest-order thermal equilibrium distribution function. These derivatives are therefore of first order in smallness. The perturbation parameter is $\lambda_{\rm mfp}/L$.

In our case, there are several simplifying approximations. As discussed in [25], the latent heat of the transition is of order $\epsilon\chi\sim(5-20)\times10^{-4}$ of the specific heat of the fluid as a whole, where $\epsilon=\delta^4/\lambda^3(30/\pi^2\mathcal{N}_{\rm eff})$ and $\chi=\lambda\gamma/\delta^2$ is the dimensionless parameter used in Sec. II. So we do not expect the temperature of the fluid as a whole to change significantly. Also, the pressure and energy of the two phases at the same temperature differ by a fraction of order $\epsilon$, so from Eq. (38) above, we expect the change in the fluid velocity across the bubble wall to be of order $\epsilon$, and therefore insignificant.

Processes which change the number of $W$ bosons include the $s$- and $t$-channel processes $W$+quark $\rightarrow$gluon+quark. Straightforward calculation of these rates in the Born approximation yields a mean $W$ lifetime $\tau\approx(4/\pi^2)(\alpha_s\alpha_W)^{-1}[1+2\ln(T/M_W)]^{-1}\approx30T^{-1}$. So to a first approximation one should treat the number of $W$'s as conserved.

This means that the zeroth-order solution has a chemical potential. Assuming number-conserving processes such as we consider below maintain good thermal contact with the fluid the $W$'s would have a constant temperature and velocity, but would develop a chemical potential across the wall. The chemical potential is easily calculated by expanding the formula for the number density $n$ in $M_W^2$ and $\mu$ and setting $n$ to be constant. One finds

$$\mu=\frac{M_W^2}{T}\frac{3}{2\pi^2}\ln(T/M_W) \tag{89}$$

which may then be used in the formula for the pressure due to collisions (84) to deduce the enhancement to the pressure caused by this buildup of $W$'s:

$$\delta P_{\rm coll}=M_W^4\frac{3}{16\pi^4}\ln^2(T/M_W) \tag{90}$$

(obtaining a factor of $\frac{1}{2}$ by integrating over $M^2$, with $\mu\propto M^2$) per $W$ degree of freedom (of which there are 9). It is then straightforward to check that in the regime of interest, this (velocity-independent) term is substantially smaller than the driving force on the wall.

One can also do the same for top quarks, which are another natural candidate for slowing the wall, being strongly coupled to the Higgs field. The analogous calculation to that above yields

$$\delta P_{\rm coll}=M_t^4\frac{3}{8\pi^4}\ln^2(2) \tag{91}$$

per top degree of freedom (of which there are 12) which is enough to stop the wall only if $M_t$ is substantially larger than $M_W$. A complication here is that the number-changing processes appear stronger than for $W$'s. For example, there is top-antitop annihilation and top+lepton/quark$\rightarrow$bottom+lepton/quark through $t$-channel $W$ exchange. The mean free time for the latter process is approximately $(1/24)(T/M_W)^2(\pi\alpha_W)^{-2}T^{-1}\sim T^{-1}$, so it is short. This means that left-handed top quarks will mix strongly with left-handed bottom quarks, eventually reducing the chemical potential for the top quarks. In addition there are strong-interaction annihilations of top quarks into gluons and light-mass quarks. The sum of these diagrams is difficult to compute with precision since it is not clear what momenta to use in the estimate—the cross section depends strongly on the momentum of the quarks, with the low-momenta quarks which dominate the collisional pressure (91) being most efficiently annihilated. The situation is further complicated by strong-interaction-induced mass gaps. We have naively estimated these effects however and find that the mean free path for annihilation appears to be less than that typical for $W$- and $Z$-boson scattering. At the end of this section we will estimate the effect of top quarks on the damping of the bubble-wall motion and argue that their effect is at best of order 1 relative to that of the $W$ and $Z$ bosons, and is probably in fact much smaller.

It is important to note that these chemical-potential-induced pressures are independent of the wall velocity, quite unlike the velocity-dependent forces of the previous section. If they stop the wall at all, they do so at zero velocity. In this situation, the wall can only propagate through particle annihilation. In the rest frame of the medium, if the particles involved have an annihilation

time $\tau$, then the wall velocity will be determined by $\gamma v \sim L/\tau$, the factor of $\gamma$ arising from Lorentz contraction of the wall width. This particle-burning limited situation is interesting, and deserves separate investigation. It may be relevant to the electroweak theory at large top-quark mass.

Since these chemical potentials are probably not enough to stop the wall, we need to examine the departures from thermal equilibrium in detail.

As argued above, we should be able to ignore shifts in the temperature and velocity of the fluid, and the chemical potential for $W$'s is small. Thus we take as our zeroth-order distribution function

$$f_0(p,x)=\frac{1}{e^{\beta\gamma_v(E-vp_x)}-1}\ , \tag{92}$$

where

$$E=\sqrt{\mathbf{p}^2+M^2(x)} \tag{93}$$

and we assume that the temperature $T$ and the velocity of the fluid $v$ may be taken to be independent of $x$.

The distribution function $f_0$ when inserted into the equation for the tadpole diagram $\eta(x)$ just produces the $\phi^3(x)$ and $\phi^4(x)$ terms in the finite-temperature effective potential. The deviations from this effective potential are given by $\delta f$.

The left-hand side of the transport equation arises from the derivative with respect to momenta and coordinate on $f_0$. A little algebra gives

$$(p\cdot\partial_x+M\mathbf{F}\cdot\nabla)f_0(p,x)=-\frac{1}{2}\beta\gamma v\frac{dM^2}{dx}\frac{e^{\beta\gamma(E-vp_x)}}{(e^{\beta\gamma(E-vp_x)}-1)^2}\ . \tag{94}$$

Now the right-hand side of the transport equation involves a scattering integral. This part of the equation involves $\delta f$.

As a function of momenta, this scattering integral is Lorentz invariant. Therefore we may Lorentz boost all momenta, holding coordinates unboosted. In these new variables, the transport equation is

$$C(x,p)=-\frac{1}{2}\beta\gamma v\frac{dM^2}{dx}\frac{e^{\beta E}}{(e^{\beta E}-1)^2}\ . \tag{95}$$

Now in the tadpole equation, we may also Lorentz boost the momenta, keeping coordinates fixed, so that the integration for $\eta(x)$ may be trivially reexpressed in terms of the boosted momenta. Therefore, we have reduced the problem of computing $\delta f$ to that for a fluid at rest in the presence of the bubble wall in its rest frame. All the thermal distribution functions will therefore be evaluated in this rest frame.

The collisional integral is

$$C(x,p_1)=-\int\frac{d^3p_2}{(2\pi)^3 2E_2}\frac{d^3p_3}{(2\pi)^3 2E_3}\frac{d^3p_4}{(2\pi)^3 2E_4}|M(s,t)|^2$$
$$\times(2\pi)^4\delta(p_1+p_2-p_3-p_4)\{f(E_1)f_2(E_2)[1\pm f_3(E_3)][1\pm f_4(E_4)]$$
$$-f_3(E_3)f_4(E_4)[1\pm f(E_1)][1\pm f_2(E_2)]\}\ . \tag{96}$$

In the above equation, the $\pm$ is plus for bosons and minus for fermions. The distribution functions $f_i$ are those appropriate for bosons or for fermions.

For the processes we consider, the $W$ and $Z$ bosons will have small masses added to them which as a function of $x$ perturb the distributions from local thermal equilibrium distributions. For high-momentum particles, these deviations are not so large, and such particles should be able to approach a solution of the transport equation by low-momentum-transfer processes. For low-energy $W$ and $Z$ bosons, the scattering will be dominantly low-momentum transfer. We therefore expect that the dominant contribution to the scattering term in the transport equation will come from low-momentum-transfer Coulombic scattering. (By Coulombic, we mean $W$- or $Z$-boson exchange.) This is the only way that the deviations from equilibrium can be parametrically small since in this case the factors of coupling constant in front of the scattering term are largely compensated by the infrared Coulomb singularity.

We now will take the expression for the collision integral and expand it to first order in small deviations from equilibrium. As discussed above, the distribution function $f(p_1,x)$ will correspond to a $W$ or $Z$ boson. The dominant process will be Coulomb scattering from fermions. We therefore take $f_3$ to correspond to a $W$ or $Z$ boson. The functions $f_2$ and $f_4$ correspond to fermions. These fermion distribution functions only change slightly due to the presence of the wall, and should be well approximated by their local equilibrium distribution functions. Expanding to first order in $\delta f$ and defining

$$\delta f(E)=\Delta(E,x)\frac{e^{\beta E}}{(e^{\beta E}-1)^2} \tag{97}$$

the transport equation becomes

$$\frac{1}{2}\frac{dM^2}{dx}\beta\gamma v=\int\frac{d^3p_2}{(2\pi)^3 2E_2}\frac{d^3p_3}{(2\pi)^3 2E_3}\frac{d^3p_4}{(2\pi)^3 2E_4}|M(s,t)|^2(2\pi)^4\delta(p_1+p_2-p_3-p_4)\frac{1+f_+^0(E_3)}{1+f_+^0(E_1)}$$
$$\times f_-^0(E_2)[1-f_-^0(E_4)][\Delta(E_1,x)-\Delta(E_3,x)]\ . \tag{98}$$

We have used $f_\pm^0$ as notation for the local thermal equilibrium distribution function for bosons and fermions respectively.

Now note that we take the temperature of the fermion fluid to be fixed—as argued above, the $W$'s will not heat it significantly. Similarly, we take the velocity of the fermion fluid to be fixed. This actually eliminates the perturbations corresponding to an overall shift in the temperature or velocity of the fluid as a whole. However, the fluid of $W$'s may independently experience a temperature or velocity shift in their distribution. The energy and momentum flux constraints in (86) are then enforced by a very small shift in the background fermion fluid temperature and velocity.

Since the collision term conserves particle number, Eq. (98) only determines the quantity $\Delta(E)$ up to an overall constant. This constant is the chemical potential for the $W$ and $Z$ bosons. Recall that as we go across the wall, inelastic particle production takes a longer time, so we ignore it.

To determine the chemical potential, we use the last equation of (86), requiring that the number density of $W$ and $Z$ bosons be conserved across the bubble wall. In the variables which have been Lorentz transformed so that the fluid is at rest, this requires that the number density of particles be constant across the bubble wall. The chemical potential is therefore determined by

$$\int d^3p\ \delta f(p,x)=0\ . \tag{99}$$

To further specify the solution to this equation, we must determine the squared matrix element $|M(s,t)|^2$. This is just the Coulomb portion of the $W$ and $Z$ scattering with the fermions. The Coulomb matrix element squared per particle from low-momentum-transfer high-energy processes is [33]

$$|M(s,t)|^2=2g^4\frac{s^2}{(t-M^2)^2} \tag{100}$$

where $g$ is the electroweak coupling strength. Now there are $N_F=48$ left-handed fermion degrees of freedom, so we define

$$\omega=2(4\pi\alpha_W)^2N_F \tag{101}$$

and

$$\eta(s,t)=\frac{s^2}{(t-M^2)^2}\ . \tag{102}$$

Defining further

$$\Delta(E,x)=\frac{1}{2\omega}\frac{dM^2}{dx}\beta^4\gamma v\kappa(E) \tag{103}$$

we can reexpress the transport equation as

$$1=\beta^3\int\frac{d^3p_2}{(2\pi)^3 2E_2}\frac{d^3p_3}{(2\pi)^3 2E_3}\frac{d^3p_4}{(2\pi)^3 2E_4}\eta(s,t)$$
$$\times(2\pi)^4\delta(p_1+p_2-p_3-p_4)\frac{[1+f_+^0(E_3)]}{[1+f_+^0(E_1)]} \tag{104}$$
$$\times f_-^0(E_2)[1-f_-^0(E_4)][\kappa(E_1)-\kappa(E_3)]\ . \tag{105}$$

Notice that in this form of the equation, all dependence on coupling, velocity, and spatial coordinates through $M^2(x)$ has disappeared. Note further that the perturbation to the distribution function is (up to a constant chemical potential) automatically zero outside the bubble wall.

The equation above is analyzed in the Appendix, where we compute the behavior of $\kappa$ at energies $E\gg M$. We have also been able to convert the twelve-dimensional integral equation for $\kappa$ into a one-dimensional integral equation with a known kernel. The derivation and analysis of this equation will be the subject of a later paper, and will not be presented here.

The contribution relevent for its effect on the equation for the scalar field is the behavior of the function $\kappa(E)$ for $E\sim T$. For this range of energy, we show in the Appendix that

$$\kappa(E)=-2(2\pi)^3\frac{E}{\ln(AE^2/M^2)}+B\ , \tag{106}$$

where $B$ is determined by the constraint that the flux of $W$ and $Z$ bosons is conserved and $A$ is an undetermined constant of order 1. We therefore find

$$\Delta(E)=-\frac{\pi}{4}\frac{1}{\alpha_W^2N_F}\frac{dM^2}{dx}\beta^4\gamma v\left[\frac{E}{\ln(AE^2/M^2)}+B\right]\ . \tag{107}$$

Notice that if we assume that $\gamma v\sim 1$, take $M\sim T/2$, take $E\sim T$, and assume the wall thickness is about $L\sim 1/\alpha_W T$, we find that $\Delta\sim\frac{1}{10}$ so that indeed the deviations from equilibrium, as far as the distribution functions are concerned, are small.

Using the condition that the flux of $W$ and $Z$ bosons is conserved, we find that

$$B\approx-\frac{3T}{\ln(AT^2/M^2)}\ . \tag{108}$$

Including a factor of 9 for the various spins and charge states of the $W$ and $Z$ bosons, we find therefore that

$$\eta(x)=\frac{9}{(16\pi)}\frac{1}{\alpha_W^2N_F}\frac{\beta\gamma v}{\ln(AT^2/M^2)}\frac{dM^2}{dx}\ . \tag{109}$$

Finally, we obtain the modification of the scalar field

equation to be

$$\frac{9}{8}(2\pi)\frac{1}{N_F}\frac{\beta\gamma v}{\ln(AT^2/M^2)}\phi^2\frac{d\phi}{dx} . \tag{110}$$

We can now use the scalar field equation to derive a virial theorem as in Eq. (45) above. Multiplying by $d\phi/dx$, integrating over $x$, and assuming that a large positive $x$ we are in the true asymmetric phase, but at large negative $x$ in the false asymmetric phase, we obtain

$$\frac{9}{8}(2\pi)\frac{1}{N_F}\frac{\beta\gamma v}{\ln(AT^2/M^2)}\int dx\,\phi^2\left[\frac{d\phi}{dx}\right]^2=-\Delta V . \tag{111}$$

In this equation, $\Delta V$ is the change in the potential energy between the phases, and is approximately

$$\Delta V\approx-\frac{\delta^4}{\lambda^3}T^4 \tag{112}$$

for $\zeta=1.6$ corresponding to the value of $\zeta$ appropriate for nucleation.

On the other hand, using the fact that for $\zeta\sim2$ the solution for the scalar field is a kink

$$\phi=\frac{\delta T}{\lambda}[1+\tanh(\sqrt{1/2\lambda}\delta T x)] \tag{113}$$

we find that

$$\beta\int dx\,\phi^2\left[\frac{d\phi}{dx}\right]^2=\frac{\delta^5}{\lambda^4}\sqrt{1/2\lambda}T^4\int dx\frac{[1+\tanh(x)]^2}{\cosh^4(x)} . \tag{114}$$

Performing the integral over $x$ gives

$$\beta\int dx\,\phi^2\left[\frac{d\phi}{dx}\right]^2=\frac{8}{5}\frac{\delta^5}{\lambda^4}\sqrt{1/2\lambda}T^4 . \tag{115}$$

Finally, combining all the terms together, we get

$$\gamma v\sim\frac{5}{27}N_F\ln(AT^2/M^2)\frac{M_H^3}{M_W^3}$$

$$\sim10\frac{M_H^3}{M_W^3} . \tag{116}$$

Using our "realistic" values for the Higgs mass, corresponding to the one-doublet-model mass 35 GeV $<M_H<$ 50 GeV, we see that the velocity is mildly relativistic, and

$$\gamma v\sim1-2 . \tag{117}$$

Due to the cubic dependence on the Higgs mass, this value could also be substantially lower if the effective value of $M_H$ were lower.

The previous expression for the bubble-wall velocity should be accepted with some caution. In the derivation we used $\zeta=1.6$, the value which is appropriate for nucleation. If we keep $\zeta$ as a free parameter, then the dependence upon the Higgs mass is much more complicated.

We can now check to see what is the magnitude of the top-quark contribution to the scalar field equation. The tadpole diagram gives

$$4g_t^2\phi(x)\eta_t(x) \tag{118}$$

where $g_t$ is the top-quark Yukawa coupling, and the factor of 4 comes from computing the trace over gamma matrices from the top-quark propagator. The function

$$\eta_t(x)=\int\frac{d^3p}{(2\pi)^3 2E}\delta f(p,X) . \tag{119}$$

We now assume that the top quark is, up to a chemical potential for the number of top quarks plus antiquarks, in local thermal equilibrium. The chemical potential for top plus antitop allows for the possibility that the annihilation diagrams may be weaker than the scattering diagrams which preserve the number of top plus antitop. The scattering diagrams should lead to mean free paths much less than typical wall sizes, but the case with annihilation and chemical equilibrium of topness is less clear.

To estimate the effect of scattering, we replace the collision term in the transport equation by

$$C(x,p)=\delta f/\tau_{\rm ann} , \tag{120}$$

where $\tau_{\rm ann}$ is the annihilation time for top quarks. The left-hand side of the transport equation is as before so that we find a chemical potential for top plus antitop to be

$$\mu_t=\frac{1}{2}\tau_{\rm ann}\beta\gamma v\frac{dM_t^2}{dx} . \tag{121}$$

This gives

$$\eta_t(x)=\frac{1}{4\pi^2}\mu_t T \tag{122}$$

which modifies the scalar field equation as

$$16\alpha_t^2 T\tau_{\rm ann}\beta\gamma v\phi^2\frac{d\phi}{dx} . \tag{123}$$

The relative magnitude of the top quark contribution to that of $W$ and $Z$ bosons is therefore

$$R\sim\frac{9\pi}{64}\frac{1}{N_F\alpha_t^2}\frac{1}{T\tau_{\rm ann}} \tag{124}$$

$$\sim\frac{15T}{\tau_{\rm ann}} . \tag{125}$$

In the above equation, we have taken $\alpha_t\sim\frac{1}{40}$. We see that the $W$ and $Z$ contributions are larger if the typical scattering length for annihilation is less than about $15/T$, which should be reasonable, but if the scattering length for annihilation is longer, then the velocity of the wall will be damped primarily by top quarks and will be less than what we have estimated.

Having determined the velocity of the phase boundary, as discussed in Sec. III, we may in principle solve for the entire pattern of fluid flow in the expanding bubble. However, since we have some fairly crude approxima-

tions on the way to our final result (117), we shall not pursue this here. A more accurate solution of the transport equation would be needed to definitively establish whether the bubble walls are detonation fronts or deflagrations. If (117) is correct, it would seem that, depending on the Higgs mass, both may well be possible, especially in multiHiggs theories.

## VII. SUMMARY AND CONCLUSION

We have seen that it is possible to compute the velocity of the bubble wall in various approximations. The best approximation is that of small departure from local equilibrium. We found an expression for the Lorentz $\gamma$ factor of the bubble wall, and it was of order unity. Unfortunately, to get a precise value involves going beyond the approximations which we made for the scattering kernel, i.e., it is dominated by low-momentum-transfer boson exchange. Since a more precise value will eventually be needed if the electroweak phase transition does generate the baryon asymmetry of the Universe, a more lengthy analysis along the lines developed in this paper would be useful.

Several qualitative results of this analysis are worth underlining:

1. The Lorentz $\gamma$ factor of the bubble wall is not enormous, so that analysis based on nonrelativistic bubble-wall propagation is probably semiquantitatively correct.

2. The bubble walls are thick. Approximations using a thin-wall bubble for computing reflection and transmission coefficients for the wall are not valid, save for exceptional tunings of parameters in a theory. To compute reflection and transmission coefficients, a WKB approximation may be good, but the difference in reflection coefficients between say a quark and an antiquark should be exponentially suppressed by $e^{-ML}$ where $M$ is the particle mass and $L$ is the bubble-wall size, except for a small range of momenta where the wavelength of the top quark is large compared to the bubble wall just at the edge of the bubble wall. In such a situation, there will be a power-law suppression of any effects associated with simultaneous reflection and transmission due to the small range of allowed phase space.

3. The motion of particles near the bubble wall is diffusive. The typical mean free path for particles with momentum close to that of the mass generated by the phase transition will in general be small compared to the wall width. Therefore, the thickness of the diffusion zone around the bubble wall is the same order as that of the wall itself. (For exceptional parameters in some models it may be possible to arrange the phase-transition temperature to be so small that the diffusive zone is larger.)

4. Due to the cubic dependence of the velocity on $M_H$, the results are sensitive to this parameter. Therefore the precise result will be sensitive to details of the Higgs potential and to as yet undetermined parameters in the theory.

## ACKNOWLEDGMENTS

Bao Hua Liu and L. McLerran would like to acknowledge support of DOE Grants Nos. DE-AC02-83ER40105 and DE-FG02-87ER40328. N. Turok acknowledges the support of NSF Contract No. PHY90-21984, the SERC (U.K.), the Alfred P. Sloan Foundation, and the David and Lucile Packard Foundation. During the writing of this manuscript, we received a preprint by M. Dine, R. Leigh, P. Huet, A. Linde, and D. Linde which overlaps to some degree our work [34]. We thank them for discussions about the similarities and differences between our works, which are in agreement for the case of thin bubbles, and in qualitative accord for thick bubbles.

## APPENDIX A: AN ANALYSIS OF THE TRANSPORT EQUATION FOR $\delta f$

In the text of the paper, we derived that the deviation from the local thermal equilibrium distribution function could be written as

$$\delta f(p,x)=\frac{1}{2\omega}\frac{dM^2}{dx}\beta^4\gamma v\frac{e^{\beta E}}{(e^{\beta E}-1)^2}\kappa(E)\ . \tag{A1}$$

The quantity $\kappa(E)$ solves the integral equation

$$1=\beta^3\int\frac{d^3p_2}{(2\pi)^3 2E_2}\frac{d^3p_3}{(2\pi)^3 2E_3}\frac{d^3p_4}{(2\pi)^3 2E_4}\eta(s,t)$$

$$\times(2\pi)^4\delta^4(p_1+p_2-p_3-p_4)\frac{[1+f_+^0(E_3)]}{[1+f_+^0(E_1)]} \tag{A2}$$

$$\times f_-^0(E_2)[1-f_-^0(E_4)][\kappa(E_1)-\kappa(E_3)]\ . \tag{A3}$$

We would like to turn this into a one-dimensional integral equation in the energy.

We begin by doing the integration over $d^3p_4$. The result is

$$1=\beta^3\int\frac{d^3p_2}{(2\pi)^3 2E_2}\frac{d^3p_3}{(2\pi)^3 2E_3}\frac{1}{2(E_1+E_2-E_3)}\frac{1+f_+^0(E_3)}{1+f_+^0(E_1)}\eta(x,t)2\pi\delta(E_1+E_2-E_3-E_4)e^{-\beta E_2}[\kappa(E_1)-\kappa(E_3)]\ . \tag{A4}$$

In this last equation, we have approximated the fermion statistical factors by their Boltzman-statistics counterparts. This should be a good approximation since the energy of the fermions will in general be large $E\sim 3T$, and here the Boltzman weight factor should be accurate to a few percent.

The integration over $|\mathbf{p}_2|$ may be done by approximating that the momentum transfer is small compared to the fermion energy. We find after some algebra that the equation becomes

$$1=\frac{\beta^3}{8(2\pi)^5}\int dp_3 d\Omega_2 d\Omega_3\frac{2p_1^2p_3^2}{(-tE_3)}\frac{1+f_+^0(E_3)}{1+f_+^0(E_1)}\eta(s,t)e^{-\beta p_2}[\kappa(E_1)-\kappa(E_3)]\ , \tag{A5}$$

where

$$p_2=\frac{-t}{2[E_1-E_3-\hat{\mathbf{p}}_2\cdot(\mathbf{p}_1-\mathbf{p}_3)]} . \tag{A6}$$

We now do an angular decomposition where

$$\hat{\mathbf{p}}_1\cdot\hat{\mathbf{p}}_2=z , \tag{A7}$$

$$\hat{\mathbf{p}}_1\cdot\hat{\mathbf{p}}_3=z' , \tag{A8}$$

$$\hat{\mathbf{p}}_2\cdot\hat{\mathbf{p}}_3=zz'+\sqrt{1-z^2}\sqrt{1-z'^2}\cos(\phi) . \tag{A9}$$

The integration over $\phi$ may now be done by the method of stationary phases expanding around the two values of $\phi$ which make $p_2$ infinite,

$$\cos(\phi_0)=\frac{E_1-E_3-p_1z+p_3zz'}{p_3\sqrt{1-z^2}\sqrt{1-z'^2}} . \tag{A10}$$

Doing the integration over $\phi$ we find that

$$1=\frac{2}{(2\pi)^4}\int dp_3dz\,dz'\frac{p_3}{E_3}\frac{1}{(t-M^2)^2}\frac{1+f_+^0(E_3)}{1+f_+^0(E_1)} \tag{A11}$$

$$\times\frac{(E_1-p_1z)^2}{\sqrt{1-z^2}\sqrt{1-z'^2}}[\kappa(E_1)-\kappa(E_3)] . \tag{A12}$$

This equation is integrated over values of $z$ and $z'$ such that the $\sin(\phi_0)$ is real.

Finally, we may do the integration over $z'$, with the result that

$$1=\frac{1}{4(2\pi)^3}\int dp_3dz\frac{p_3^2}{E_3|\mathbf{p}_3-\mathbf{p}_1|^5}\frac{1+f_+^0(E_3)}{1+f_+^0(E_1)}\frac{t}{(t-M^2)^2}[t(E_1+E_3)^2-2p_1^2p_3^2(1-z^2)][\kappa(E_1)-\kappa(E_3)] . \tag{A13}$$

This equation can be integrated over $z$ to obtain a one-dimensional integral equation for $\kappa(E)$. We are here however interested only in processes which involve small momentum transfer. If large momentum transfer is involved, then our approximations are incorrect. We will also see that the solution to this equation for $\kappa(E)$ goes like $E$ for large $E$ up to logarithms of $E$. Therefore in the integrations in the tadpole contribution the dominant contribution arises for energies much larger than $M$. In this case, we expect that the momentum transfers will be small compared to the energies of either the fermions or the $W$ and $Z$ bosons. To get the leading contribution to the above equation, we may therefore write $\mathbf{p}_3=\mathbf{p}_1+\mathbf{q}$ and expand for small $q$. Upon changing variables from $p_3$ to $q$, we find

$$1=\frac{1}{4(2\pi)^3}\int dq\,dz\frac{1}{E'q^3}\frac{1+f_+^0(E')}{1+f_+^0(E)}\frac{t'}{(t'-M^2)^2}$$

$$\times\{t'(E+E')^2+\tfrac{1}{2}(E+E')^2(E-E')^2-q^2[p^2+(\mathbf{p}+\mathbf{q})^2]+\tfrac{1}{2}q^4\}[\kappa(E)-\kappa(E')] , \tag{A14}$$

where

$$E'=\sqrt{(\mathbf{p}+\mathbf{q})^2+M^2} , \tag{A15}$$

$$t'=2M^2+2\mathbf{p}^2+2\mathbf{p}\cdot\mathbf{q}-2EE' . \tag{A16}$$

If we expand up to and including terms of second order in $q$, the equation for $\kappa$ becomes after much algebra

$$1=\frac{3}{8(2\pi)^3}\int dq^2dz\frac{q^2}{q^2+M^2}\left\{\left[-1+z^2\left[1+\frac{2\beta E_p}{e^{\beta E_p}-1}\right]-\frac{4z^2M^2}{q^2+M^2}\right]\frac{d\kappa}{dE_p}+E_pz^2\frac{d^2\kappa}{dE^2}\right\} . \tag{A17}$$

In this equation, the upper limit of integration should be taken as of order $E_p$, since when $q$ becomes of this order, all of the approximations we have used assuming the dominance of low-momentum-transfer Coulombic processes breaks down. Fortunately, the integral, although logarithmically divergent at the upper end, gets its contribution to leading order in logarithms of energy from the region of integration where

$$M\ll q\ll E_p \tag{A18}$$

so that our analysis is consistent.

Performing the integrations over $q$ and $z$ gives a differential equation for $\kappa$:

$$1=-\frac{1}{2(2\pi)^3}\ln(E^2/M^2)\left[\left[1-\frac{\beta E}{e^{\beta E}-1}\right]\frac{d\kappa}{dE}-\frac{E}{2}\frac{d^2\kappa}{d^2E}\right] . \tag{A19}$$

For energies $M \ll E \ll T$, the solution to this equation to leading order in $\ln(E)$ is

$$\kappa(E)=4(2\pi)^3\ln[A\ln B(E/M)]+C . \tag{A20}$$

Here $A$ and $C$ are integration constants which are formally undetermined in this energy region but do not affect the asymptotic solution. The constant $B$ reflects the uncertainty over the precise value of the cutoff in the integration over $q$. This contribution is largest for large energy.

In fact the dominant contribution to the equation for the scalar field arises for $E \sim T$. In this case, to leading order in logarithms

$$\kappa(E)=-2(2\pi)^3\frac{E}{\ln(AE^2/M^2)}+B . \tag{A21}$$

In this equation the constant $B$ is an integration constant which does not affect the asymptotic behavior. Its values is determined by requiring that the flux of $W$ and $Z$ bosons is conserved across the bubble wall. The constant $B$ reflects the ambiguity associated with properly determining the cutoff in the integration over $q$, and also does not affect the asymptotic nature of $\kappa$.


[1] G. 't Hooft, Phys. Rev. Lett. **37**, 8 (1976); Phys. Rev. D **14**, 3432 (1976).

[2] A. Linde, Phys. Lett. **70B**, 306 (1977).

[3] S. Dimopoulos and L. Susskind, Phys. Rev. D **18**, 4500 (1978).

[4] N. Manton, Phys. Rev. D **28**, 2019 (1983).

[5] F. Klinkhamer and N. S. Manton, Phys. Rev. D **30**, 2212 (1984).

[6] V. A. Kuzmin, V. A. Rubakov, and M. E. Shaposhnikov, Phys. Lett. **155B**, 36 (1985).

[7] P. Arnold and L. McLerran, Phys. Rev. D **36**, 581 (1987); **37**, 1020 (1988).

[8] For a clear review, see M. Mattis, Phys. Rep. **214**, 159 (1992).

[9] L. Carlson, Xu Li, L. McLerran, and R. T. Wang, Phys. Rev. D **42**, 2127 (1990).

[10] A. D. Sakharov, Pis'ma Zh. Eksp. Teor. Fiz. **5**, 32 (1967) [JETP Lett. **5**, 24 (1967)]; V. A. Kuzmin, *ibid.* **13**, 335 (1970) [**13**, 228 (1970)]; A. Yu. Ignatiev, N. V. Krasnikov, V. A. Kuzmin, and A. N. Tavkhelidze, in *Neutrino '77*, Proceedings of the International Conference on Neutrino Physics and Neutrino Astrophysics, Balesan Valley, U.S.S.R., 1977, edited M. A. Markov, G. V. Domogatsky, A. A. Komar, and A. N. Tavkhelidze (Nauka, Moscow, 1978), Vol. 2, p. 293; Phys. Lett. **76B**, 436 (1978); M. Yoshimura, Phys. Rev. Lett. **41**, 281 (1978); **42**, 476(E) (1979); S. Weinberg, *ibid.* **42**, 850 (1979); A. Yu. Ignatiev, V. A. Kuzmin, and M. E. Shaposhnikov, Phys. Lett. **87B**, 114 (1979).

[11] D. A. Kirzhnits and A. Linde, Ann. Phys. (N.Y.) **101**, 195 (1976).

[12] I. Affleck, Phys. Rev. Lett. **46**, 388 (1981).

[13] A. Bochkarev and M. Shaposhnikov, Mod. Phys. Lett. A **2**, 417 (1987).

[14] N. Turok and J. Zadrozny, Nucl. Phys. **B369**, 729 (1992).

[15] M. Carrington, Phys. Rev. D **45**, 2933 (1992).

[16] M. Dine, R. G. Leigh, P. Huet, A. Linde, and D. Linde, Phys. Rev. D **46**, 550 (1992).

[17] M. E. Shaposhnikov, Pis'ma Zh. Eksp. Teor. Fiz. **44**, 364 (1986) [JETP Lett. **44**, 465 (1986)]; Nucl. Phys. **B287**, 757 (1987); **B299**, 797 (1988); A. I. Bochkarev, S. Yu. Khlebnikov, and M. E. Shaposhnikov, *ibid.* **B329**, 493 (1990).

[18] L. McLerran, Phys. Rev. Lett. **62**, 1075 (1989).

[19] A. D. Cohen, D. B. Kaplan, and A. E. Nelson, Phys. Lett. B **246**, 561 (1990); **349**, 727 (1991).

[20] N. Turok and J. Zadrozny, Phys. Rev. Lett. **65**, 2331 (1990); Nucl. Phys. **B358**, 471 (1991).

[21] L. McLerran, M. Shaposhnikov, N. Turok, and M. Voloshin, Phys. Lett. B **256**, 561 (1991).

[22] M. Dine, P. Huet, R. Singleton, and L. Susskind, Phys. Lett. B **257**, 351 (1991).

[23] A. G. Cohen, D. B. Kaplan, and A. E. Nelson, Phys. Lett. B **263**, 86 (1991).

[24] M. Shaposhnikov, Phys. Lett. B **277**, 324 (1992).

[25] A. D. Linde, Nucl. Phys. **B216**, 421 (1983).

[26] N. Turok, Phys. Rev. Lett. **68**, 1803 (1992).

[27] P. Steinhardt, Phys. Rev. D **25**, 2074 (1982).

[28] M. Gyulassy, Nucl. Phys. **B237**, 477 (1984).

[29] K. Enqvist, J. Ignatius, K. Kajantie, and K. Rummukainen, Phys. Rev. D **45**, 3415 (1992).

[30] D. B. Kaplan and A. E. Nelson (private communication).

[31] K. Freese and F. C. Adams, Phys. Rev. D **41**, 2449 (1990).

[32] D. Grigoriev, M. Shaposhnikov, and N. Turok, Phys. Lett. B (to be published).

[33] S. de Groot, A. van Leuwen, and C. G. van Weert, *Relativistic Kinetic Theory* (North-Holland, Amsterdam, 1980).

[34] D. W. Oertzen, University of Cape Town Report No. UCT-TP-158/90, 1990 (unpublished).